UNIVERSIDADE FEDERAL DE MINAS GERAIS
INSTITUTO DE CIÊNCIAS BIOLÓGICAS
DEPARTAMENTO DE MORFOLOGIA
PROGRAMA DE PÓS-GRADUAÇÃO
EM BIOLOGIA CELULAR

TESE DE DOUTORADO

AVALIAÇÃO DA REMODELAÇÃO OVARIANA PÓS-DESOVA DA TILÁPIA-DO-NILO (*OREOCHROMIS NILOTICUS*) EM CONDIÇÕES DE CULTIVO

RAFAEL MAGNO COSTA MELO

Belo Horizonte

2014

Rafael Magno Costa Melo

Avaliação da remodelação ovariana pós-desova da tilápia-do-nilo (*Oreochromis niloticus*) em condições de cultivo

Tese de Doutorado apresentada ao Programa de Pós-graduação em Biologia Celular da Universidade Federal de Minas Gerais como requisito para a obtenção do título de Doutor.

Belo Horizonte
Instituto de Ciências Biológicas – UFMG
2014

Universidade Federal de Minas Gerais - Instituto de Ciências Biológicas
Programa de Pós-Graduação em Biologia Celular

ATA DA DEFESA DE TESE DE DOUTORADO DE

RAFAEL MAGNO COSTA MELO

126/2014/06
entrada
2°/2010
2010720800

Às **quatorze horas** do dia **06 de junho de 2014**, reuniu-se, no Instituto de Ciências Biológicas da UFMG, a Comissão Examinadora da Tese, indicada pelo Colegiado de Programa, para julgar, em exame final, o trabalho final intitulado: **"AVALIAÇÃO DA REMODELAÇÃO OVARIANA PÓS-DESOVA DA TILÁPIA-DO-NILO (*OREOCHROMIS NILOTICUS*)"** requisito final para obtenção do grau de Doutor em Biologia Celular, área de concentração: **Biologia Celular.** Abrindo a sessão, o Presidente da Comissão, **Dr. Nilo Bazzoli**, após dar a conhecer aos presentes o teor das Normas Regulamentares do Trabalho Final, passou a palavra ao candidato, para apresentação de seu trabalho. Seguiu-se a arguição pelos examinadores, com a respectiva defesa do candidato. Logo após, a Comissão se reuniu, sem a presença do candidato e do público, para julgamento e expedição de resultado final. Foram atribuídas as seguintes indicações:

Prof./Pesq.	Instituição	Indicação
Dr. Nilo Bazzoli (Orientador)	UFMG	aprovada
Dra. Elizete Rizzo (Co-orientadora)	UFMG	aprovada
Dr. Hélio Batista dos Santos	UFSJ	aprovada
Dr. Fábio Pereira Arantes	PUC - MG	aprovada
Dr. Ronald Kennedy Luz	UFMG	aprovada
Dr. Hélio Chiarini Garcia	UFMG	aprovada

Pelas indicações, o candidato foi considerado: aprovado

O resultado final foi comunicado publicamente ao candidato pelo Presidente da Comissão. Nada mais havendo a tratar, o Presidente encerrou a reunião e lavrou a presente ATA, que será assinada por todos os membros participantes da Comissão Examinadora. **Belo Horizonte, 06 de junho de 2014.**

Dr. Nilo Bazzoli (Orientador) _____

Dra. Elizete Rizzo (Co-orientadora) _____

Dr. Hélio Batista dos Santos _____

Dr. Fábio Pereira Arantes _____

Dr. Ronald Kennedy Luz _____

Dr. Hélio Chiarini Garcia _____

Obs: Este documento não terá validade sem a assinatura e carimbo do Coordenador

SECRETARIA DA PÓS-GRADUAÇÃO EM BIOLOGIA CELULAR
ICB - UFMG

Esta tese foi realizada no Laboratório de Ictiohistologia do Departamento de Morfologia da Universidade Federal de Minas Gerais (UFMG), Laboratório de Aquacultura da Escola de Veterinária da UFMG e Laboratório de Ictiologia do Programa de Pós-Graduação em Zoologia de Vertebrados da Pontifícia Universidade Católica de Minas Gerais.

ORIENTADOR:

PROF. DR. NILO BAZZOLI

CO-ORIENTADORA:

PROFA. DRA. ELIZETE RIZZO

APOIO FINANCEIRO E INSTITUCIONAL:

- Coordenação de Aperfeiçoamento de Pessoal de Nível Superior (CAPES);
- Conselho Nacional de Desenvolvimento Científico e Tecnológico (CNPq);
- Fundação de Amparo à Pesquisa do Estado de Minas Gerais (FAPEMIG);
- Centro de Microscopia da UFMG;
- Centro de Aquisição e Processamento de Imagens (CAPI) da UFMG.

AGRADECIMENTOS

Ao Dr. Nilo Bazzoli, pela orientação, ensinamentos, amizade e crescimento profissional proporcionado ao longo de mais de 10 anos de convivência;

À Dra. Elizete Rizzo pela precisa co-orientação e oportunidade em integrar a equipe do Laboratório de Ictiohistologia da UFMG;

Aos pesquisadores Dr. Ronald Kennedy Luz e Yuri Simões Martins pela significativa colaboração e contribuição ao trabalho;

À Mônica, pela amizade, agradável convivência e confecção das lâminas histológicas;

Aos pesquisadores Paulo Henrique de Almeida Campos-Junior, Dr. Hélio Batista dos Santos e Dr. Ralph Gruppi Thomé pelo valioso suporte durante a execução do estudo;

Aos técnicos e professores do Laboratório de Aquacultura da Escola de Veterinária da UFMG, em especial à Érika e ao Gabriel, pela assistência durante a coleta do material;

Aos técnicos do Centro de Microscopia da UFMG, em especial à Roberta e ao Kinulpe, pelo auxílio durante as etapas de microscopia eletrônica do material;

A todos os amigos e companheiros de trabalho do Laboratório de Ictiohistologia da UFMG, em especial à Paula, Violeta, Fabrício, Yves, Davidson, Luis, André Weber, Guto, Letícia, Claudinha e demais pessoas que por ali passaram;

Aos professores e funcionários do Programa de Pós-graduação em Biologia Celular da UFMG;

Aos professores e funcionários do Programa de Pós-graduação em Zoologia da PUC Minas;

À Marina, meu amor, meu porto seguro, minha fonte de inspiração, nosso crescimento profissional juntos foi muito importante;

À minha família, em especial a minha querida mãe Léa e minha tia Alcinéa, e amigos, pelo constante apoio e incentivo profissional;

Aos mistérios da vida, em especial às ciências naturais e aos peixes, pela permanente inquietação intelectual e pelo prazer em investigar, descobrir e contribuir com conhecimento para um mundo menos inóspito aos seres vivos.

SUMÁRIO

Resumo

As tilápias constituem o segundo grupo mais importante de peixes cultivados na aquacultura mundial e a tilápia-do-nilo, *Oreochromis niloticus* (Linnaeus, 1758), é a principal espécie de tilápia cultivada atualmente. Estudos sobre a recuperação ovariana após desova em espécies de importância comercial, como *O. niloticus*, fornecem importantes parâmetros reprodutivos para o cultivo das espécies. Ovários de peixes após a desova também são excelentes modelos experimentais para estudar mecanismos de morte celular programada, especialmente devido à remodelação tecidual que envolve crescimento e regressão folicular para início de novo ciclo reprodutivo. Desta forma, o presente trabalho teve como principal objetivo avaliar a dinâmica de remodelação ovariana da tilápia-do-nilo após a desova em cativeiro. Inicialmente, foi avaliada a dinâmica morfológica e quantitativa do crescimento folicular após desova, e posteriormente, o papel da apoptose e autofagia no crescimento e regressão folicular pós-desova em ovários de *O. niloticus*. Amostras ovarianas foram coletadas semanalmente, no período entre 0 a 24 dias pós-desova, para análises histológicas, ultraestruturais, TUNEL *in situ*, imunofluorescência (caspase-3) e morfométricas. Ovários recém-desovados continham folículos em todos os estádios de desenvolvimento, com predominância de folículos em crescimento primário inicial (~42%) e folículos de crescimento completo (~20%). Folículos pós-ovulatórios representaram cerca de 5% dos folículos ovarianos logo após a desova, e menos de 1% após 7 dias. Folículos atrésicos representaram cerca de 2% dos folículos durante o período de estudo. Folículos em crescimento primário mantiveram um estoque estável durante a remodelação ovariana, indicando disponibilidade para recrutamento contínuo. Vinte e um dias pós-desova, os folículos de crescimento completo predominaram nos ovários, representando cerca de 35% dos folículos. Todos os folículos, exceto pós-ovulatórios e atrésicos, cresceram em tamanho significativamente ao longo da remodelação ovariana. A ultraestrutura dos folículos em crescimento revelou uma intensa atividade de

síntese das células foliculares, as quais contribuíram ativamente para a formação da zona radiata e desenvolvimento ovocitário após desova. Os resultados mostraram uma rápida recuperação ovariana e crescimento folicular de *O. niloticus*, em 21 dias a 29,5 °C, para permitir a próxima desova. A segunda etapa do trabalho revelou, durante o crescimento folicular pós-desova, uma baixa ocorrência de apoptose nas células foliculares e tecais dos folículos. Logo após a desova, folículos pós-ovulatórios exibiram células foliculares hipertrofiadas com intensa atividade de síntese, altas taxas de apoptose folicular e início de autofagia para depuração celular. Folículos pós-ovulatórios, 7 dias pós-desova, mostraram células foliculares com abundante maquinaria autofágica e menor apoptose folicular. Folículos atrésicos iniciais mostraram células foliculares hipertrofiadas contendo numerosas organelas de síntese, intensa atividade heterofágica para fagocitose do vitelo e baixa taxa de apoptose folicular. Na atresia avançada, o vitelo foi quase todo fagocitado pelas células foliculares, que exibiram diminuição da atividade de síntese acompanhada pelo aumento de autofagia e apoptose folicular. Nos folículos atrésicos finais, as células foliculares apresentaram citoplasma marcadamente eletron-lúcidos e aumento da apoptose. Estes resultados indicaram que autofagia e apoptose agem cooperativamente para uma eficiente regressão e eliminação dos folículos pós-ovulatórios e atrésicos em ovários de tilápia-do-nilo. Adicionalmente, a apoptose exerce um importante papel na homeostase do folículo ovariano em crescimento após a desova.

PALAVRAS-CHAVE: ovário, peixe, reprodução, regeneração ovariana, crescimento folicular, regressão folicular, apoptose, autofagia.

Abstract

Tilapias are the second most important group of fish cultivated in aquaculture worldwide and the Nile tilapia *Oreochromis niloticus* (Linnaeus, 1758) is the main species of tilapia currently farmed. Studies about the ovarian regeneration after spawning in species of commercial importance, such as *O. niloticus*, provides important reproductive parameters for the cultive of the species. Fish ovaries after spawning are also excellent experimental models for studying mechanisms of programmed cell death, especially due to tissue remodeling involving follicular growth and regression for initiation of new reproductive cycle. Thus, the present study aimed to evaluate the dynamics of ovarian remodeling of Nile tilapia after spawning in captivity. To achieve this goal, ovarian samples were collected weekly for histological, ultrastructural, in situ TUNEL, immunohistochemistry (caspase 3) and morphometric analysis. Initially, the quantitative and morphological dynamics of follicular growth after spawning was evaluated, and then, the role of apoptosis and autophagy was studied during follicular growth and regression after spawning in *O. niloticus* ovaries. Recently spawned ovaries contained follicles at all stages of development, with a predominance of early primary growth (~42%) and full-grown follicles (~20%). Post-ovulatory follicles represented approximately 5% of the ovarian follicles after spawning, and less than 1% after 7 days. Atretic follicles accounted for approximately 2% of the follicles during the study period. Primary growth follicles maintained a stable stock during ovarian remodeling, indicating their availability for continuous recruitment. Twenty-one days after spawning, the full-grown follicles predominated in the ovaries, representing approximately 35% of the follicles. All follicles, except post-ovulatory and atretic, grew significantly along the ovarian remodeling. The ultrastructure of growing follicles revealed an intense synthesis activity of the follicular cells, which actively contributed to formation of the zona radiata and oocyte development after spawning. The results showed a rapid ovarian recovery and

follicular growth of *O. niloticus*, in 21 days at 29.5°C, to allow the next spawning. The second stage of the present work revealed, during follicular growth after spawning, a low occurrence of apoptosis in the follicular cells and theca of the follicles. Shortly after spawning, post-ovulatory follicles exhibited hypertrophied follicular cells with intense synthesis activity, high rates of follicular apoptosis and autophagy to cell clearance. Post-ovulatory follicles, 7 days post-pawning, showed follicular cells with abundant autophagic machinery and lower apoptosis. Early atretic follicles showed follicular cells containing numerous synthesis organelles, heterophagous activity for phagocytosis of the yolk and low apoptosis. In advanced atresia, the yolk continues to be phagocytosed by the follicular cells, which exhibited decreased synthesis activity accompanied by increased apoptosis and autophagy. In late atretic follicles, the follicular cells presented a markedly electron-lucid cytoplasm and increased apoptosis. These results indicate that autophagy and apoptosis act cooperatively for efficient regression and elimination of post-ovulatory and atretic follicles in ovaries of Nile tilapia and are essential mechanisms in ovarian remodeling post-spawning. Additionally, apoptosis plays an important role in the homeostasis of growing follicles after spawning.

KEYWORDS: ovary, fish, reproduction, ovarian regeneration, follicular growth, follicular regression, apoptosis, autophagy.

1- INTRODUÇÃO E JUSTIFICATIVA

As tilápias constituem o segundo grupo mais importante de peixes cultivados na aquacultura mundial e a tilápia-do-nilo *Oreochromis niloticus* (Linnaeus, 1758) é a principal espécie de tilápia cultivada atualmente (FAO, 2014). Além disto, a tilápia-do-nilo constitui um importante modelo experimental para estudos de biologia da reprodução devido à desova em diversas condições ambientais, adaptabilidade a diversos sistemas de cultura e resistência a doenças e infecções (Coward & Bromage, 2000; Little & Hulata, 2000). Estudar a dinâmica de remodelação ovariana após desova em peixes, especialmente em espécies de importância comercial como *O. niloticus*, é importante para fornecer parâmetros reprodutivos para o aprimoramento do cultivo das espécies.

Ovários de peixes após a desova também são excelentes modelos experimentais para estudar mecanismos de morte celular programada e autofagia, especialmente devido à remodelação tecidual que envolve crescimento e regressão folicular para início de um novo ciclo reprodutivo (Santos et al., 2005; Thomé et al., 2012; Morais et al., 2012). Devido à conservação evolutiva de uma ampla gama de proteínas e processos envolvidos na morte celular, ovários de peixes podem fornecer informações valiosas para compreender diversas doenças e mecanismos biológicos em vertebrados (Kerr et al., 1972; Hussein, 2005; Degterev & Yuan, 2008; Bolt & Klimecki, 2012).

1.1- A TILÁPIA-DO-NILO (*OREOCHROMIS NILOTICUS*)

A tilápia-do-nilo *O. niloticus* (Figura 1) pertence à ordem Perciformes, família Cichlidae e subfamília Tilapiinae (Nagl et al., 2001). As áreas de distribuição geográfica natural de *O. niloticus* são as bacias dos rios Nilo, Níger e Senegal (leste e oeste da África), sendo a partir destes locais amplamente introduzidas para o cultivo no Oriente Médio, Sudoeste Asiático, Estados Unidos e América do Sul (Popma & Lovshin, 1996). Atualmente, as tilápias constituem um dos grupos mais importantes de peixes cultivados na aquacultura

mundial. A tilápia-do-nilo é a principal espécie de tilápias cultivada, com uma produção estimada em 2010 de 2.5 milhões de toneladas e valor de mercado superior a US$ 4 bilhões (FAO, 2014).

Figura 1. Espécie de estudo: *Oreochromis niloticus* (Linnaeus, 1758). Escala: 1 cm

Dentre as características que tornam as tilápias atraentes para aquacultura, pode-se destacar a excelente qualidade de sua carne, o crescimento e reprodução em diversas condições ambientais, a resistência a doenças e infecções e a tolerância ao estresse induzido pelo manejo (Little & Hulata, 2000). Além disso, a precocidade sexual e a capacidade de reproduzir durante todo o ano em locais com temperatura acima de 24ºC garantem uma grande disponibilidade de alevinos para o cultivo (Lund & Figueira, l989). Na natureza, a tilápia-do-nilo atinge a primeira maturação sexual a partir de 20 cm e em cativeiro com 10 a 17 cm de comprimento (Leonhardt, 1997). Em regiões tropicais ou em condições adequadas de cultivo, a fêmea desova de 1.500 a 2.000 ovos por vez e o intervalo entre duas desovas consecutivas ocorre a cada 3 ou 4 semanas (Jalabert & Zohar, 1982; Lund & Figueira, 1989; Tacon et al., 1996; Coward & Bromage, 2000). A tilápia-do-nilo possui desenvolvimento ovariano do tipo assincrônico e grande variabilidade na frequência de desova mesmo em condições ambientais controladas (Coward & Bromage, 1999). O intervalo entre desovas

(ISI) também pode ser influenciado pelo tamanho, idade, estado nutricional e linhagem do peixe, assim como pela densidade de estocagem, proporção sexual, temperatura e fotoperíodo (Gunasekera et al., 1996; Ridha & Cruz, 1999; Little & Hulata, 2000; Campos-Mendoza et al., 2004). A frequência de desova entre tilápias também pode ser influenciada pela interação social, estímulos audíveis e químicos de seus conespecíficos (Coward & Bromage, 2000).

Apesar da tilápia-do-nilo figurar entre as cinco espécies mais importantes comercialmente na aquacultura em todo mundo (FAO, 2014), a baixa produtividade dos reprodutores representa a restrição mais significativa sobre a produção comercial de tilápias (Coward & Bromage, 2000; Little & Hulata, 2000). Desta forma, aumentar o conhecimento sobre a biologia reprodutiva de reprodutoras é importante para o aprimoramento do cultivo da espécie.

1.2- FOLICULOGÊNESE E CRESCIMENTO FOLICULAR

Em peixes teleósteos, o desenvolvimento dos folículos ovarianos é regulado hormonalmente pelo eixo hipotálamo-hipófise-gônada. Sinais ambientais, em conjunto com os estímulos sociais, são convertidos em informações sensoriais no hipotálamo, que estimula a produção de hormônios liberadores de gonadotropinas (GnRH). Estes hormônios atuam sobre a adenohipófise, que sintetiza os hormônios gonadotróficos folículo estimulante (FSH) e luteinizante (LH). A dopamina secretada pelo hipotálamo pode inibir a liberação de LH. Os hormônios FSH e LH irão estimular as gônadas a produzir os hormônios sexuais esteroides 17β estradiol (E2) e 17β, 20α dihidroxi-4-pregnen-3-one (17β-20α DHP). Em fêmeas, o E2 promove a proliferação das ovogônias e vitelogênese, enquanto 17β-20α DHP é responsável pelo início da meiose das células germinativas, maturação ovocitária e ovulação (Lubzens et al., 2010; Yaron & Levavi-Sivan, 2011) (Figura 2).

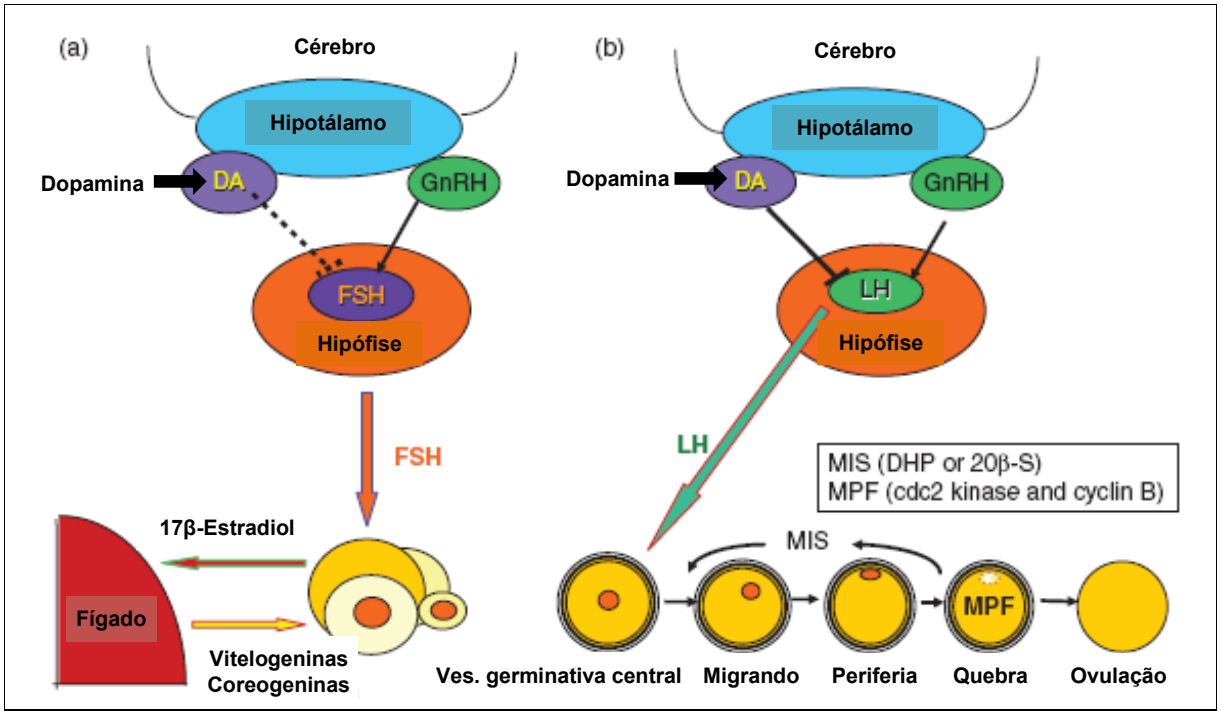

Figura 2. Modelo do eixo hipotálamo-hipófise-gônada em fêmeas: a) durante a vitelogênese e b) durante a maturação final ovocitária e ovulação (Yaron & Levavi-Sivan, 2011).

A foliculogênese se inicia com a proliferação e diferenciação das células germinativas primordiais em ovogônias, que se encontram no epitélio germinativo que margeia a lamela ovariana (Grier et al., 2009). A ovogônia-A não diferenciada divide por mitose originando ovogônia-A diferenciada que prolifera para gerar ovogônia-B, iniciando a formação de cistos germinativos. Dentro dos cistos, ovogônia-B entra em meiose tornando-se ovócitos (Quagio-Grassiotto et al., 2011). Quando a foliculogênese é completada, o folículo ovariano, que compreende um ovócito e as células foliculares envoltórias, é circundado por uma membrana basal e células da teca, resultando na formação de um complexo folicular (Grier, 2012).

Durante o crescimento folicular existem duas fases distintas: crescimento primário e crescimento secundário (Lubzens et al., 2010). O crescimento primário é caracterizado por uma intensa proliferação de organelas, diferenciação das células foliculares e tecais, início da formação da zona radiata e acúmulo de alvéolos corticais na periferia do ooplasma. No fígado, o E2 estimula os hepatócitos a produzirem vitelogenina e coreogenina, que são levadas pela corrente sanguínea até o ovário, onde participam na formação do vitelo e no

desenvolvimento da zona radiata, iniciando o crescimento secundário (Figura 2). A vitelogenina leva a rápida acumulação de glóbulos de vitelo no ovócito e grande aumento no diâmetro dos folículos, principalmente durante a prófase I da meiose (Tyler & Sumpter, 1996; Patiño & Sullivan, 2002). O processo de maturação final do folículo, que ocorre durante a metáfase II da meiose, caracteriza-se pela migração da vesícula germinativa ao polo animal do folículo e formação da micrópila, culminando com a ovulação e desova (Lubzens et al., 2010) (Figura 3).

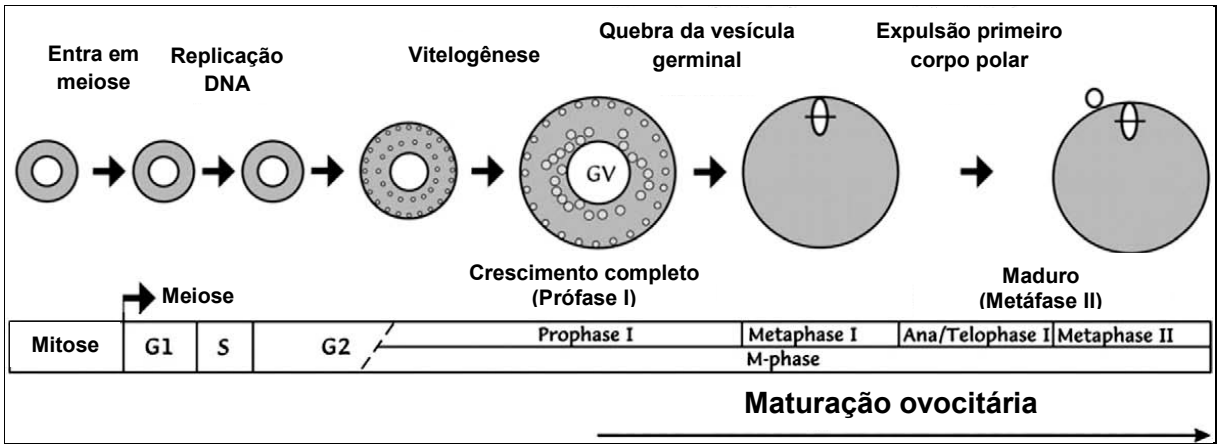

Figura 3. Esquema do desenvolvimento folicular em relação à mitose e meiose desde os ovócitos primários até a maturação final em peixes (Lubzens et al., 2010).

1.3- REGRESSÃO FOLICULAR APÓS DESOVA

Após a desova, ocorre uma remodelação tecidual em ovários de peixes para início de um novo ciclo reprodutivo, cuja escala temporal de regeneração ovariana varia de acordo com a estratégia reprodutiva da espécie. Espécies com desova total, cujos ovócitos se desenvolvem em grupos-sincrônicos para desova em um curto período reprodutivo, apresentam uma lenta regressão e regeneração dos ovários (Leonardo et al., 2006; Santos et al., 2008a). Espécies com desova parcelada, que possuem desenvolvimento assincrônico dos ovócitos para desova durante um prolongado período reprodutivo, a regeneração ovariana é rápida e dinâmica, mas com variações temporais entre os extremos desta estratégia reprodutiva (Coward & Bromage, 1998; Andrade et al., 2001; Melo et al., 2014).

Indicadores do sucesso reprodutivo nos ovários, os folículos pós-ovulatórios (FPO) são compostos de uma membrana basal que separa as células foliculares da teca e são rapidamente reabsorvidos durante a involução folicular (Thomé et al., 2006; Santos et al., 2008b). Os folículos vitelogênicos que não são desovados durante o período reprodutivo tornam-se folículos atrésicos (FA) e são reabsorvidos em um processo fisiológico prolongado, conhecido como atresia folicular (Santos et al., 2008a; Thomé et al., 2009). Após a desova, FPO e FA regridem progressivamente e os ovários exibem uma remodelação tecidual para início de um novo ciclo reprodutivo.

Vários estudos têm mostrado a contribuição de mecanismos de morte celular em ovários de peixes após desova (Drummond et al., 2000; Santos et al., 2005; Thomé et al., 2009; Morais et al., 2012). Além disto, a apoptose é citada como o principal mecanismo envolvido na eliminação de células somáticas e germinativas durante a involução de folículos ovarianos em aves (Murdoch et al., 2005; Sundaresan et al., 2007) e em mamíferos (Rolaki et al., 2005; Luz et al., 2006; Matsuda et al., 2012).

1.4- MORTE CELULAR EM OVÁRIOS DE PEIXES

A sobrevivência dos organismos multicelulares deve-se a interação entre as diversas linhagens celulares existentes, onde o controle do número de células é obtido através do balanço entre proliferação e morte celular (Thompson, 1995). A morte celular programada é um processo ativo regulado geneticamente que elimina as células desnecessárias ou danificadas durante o desenvolvimento e homeostase de organismos multicelulares (Kerr et al., 1972; Jenkins et al., 2013). Evidências obtidas a partir de vários modelos mostram que múltiplos programas de morte celular podem ser desencadeados dependendo das circunstâncias envolvidas no contexto celular (Assunção Guimarães & Linden, 2004; Degterev & Yuan, 2008).

A apoptose afeta células individualizadas que se destacam das células vizinhas e da membrana basal. Este tipo de morte celular, altamente conservado durante a evolução, é caracterizado principalmente pela fragmentação do DNA internucleosomal formando corpos apoptóticos, que são endocitados por fagócitos profissionais ou células vizinhas, evitando, desta forma, uma reação inflamatória (Bangs et al., 2000; Djavaheri-Mergny et al., 2010). A apoptose é comumente detectada através de características morfológicas, tais como o encolhimento e perda de adesão da célula e a condensação da cromatina em um padrão crescente subjacente ao envelope nuclear (Santos et al., 2005; Santos et al., 2008a). Os principais efetores da morte celular programada são caspases que ativam endonucleases dependentes-Ca^{2+}/Mg^{2+}, as quais clivam o DNA em fragmentos de 180-200 pares de bases. Dentre as caspases, caspase-3 é uma molécula efetora chave do programa apoptótico, responsável pela clivagem proteolítica de uma ampla gama de proteínas celulares que levam às características mudanças morfológicas da apoptose (Huettenbrenner et al., 2003).

A autofagia é um complexo programa catabólico geneticamente regulado e conservado evolucionariamente desde levedura até mamíferos. Sua principal função é a reciclagem de organelas citoplasmáticas e proteínas danificadas através da maquinaria lisossomal (Cao & Klionsky, 2007; Santos et al., 2008b; Kang et al., 2011). Em adição à provável contribuição na morte celular, autofagia é primariamente um mecanismo de sobrevivência de células famintas usualmente utilizadas para gerar ambos nutrientes e energia para manter a viabilidade celular (Debnath et al., 2005). O acúmulo de vacúolos autofágicos no citoplasma, repletos com organelas e materiais citoplasmáticos como mitocôndrias, ribossomos e retículos endoplasmáticos, é uma das principais características morfológicas da autofagia (Lockshin & Zakeri, 2004; Nixon et al., 2007).

A relação entre apoptose e autofagia é complexa, em algumas circunstâncias, autofagia é uma forma de adaptação ao estresse celular por suprimir a apoptose, enquanto em

outras condições, pode induzir as diferentes vias de sinalização de morte celular (Mizushima et al., 2008; Maiuri et al., 2010). A autofagia possui funções específicas e dependentes do contexto na morte celular, podendo promover tanto a morte celular por apoptose dependente-caspases e morte celular não apoptótica quando as caspases são inibidas (Lockshin & Zakeri, 2004; Denton et al., 2012). A interação de beclin-1 com a proteína anti-apoptótica bcl-2 é crucial na determinação do destino celular, e o cruzamento entre autofagia e apoptose é promovido pela clivagem de beclin-1 mediada pela caspase (Klionsky, 2007; Kang et al., 2011). Em ovários de teleósteos, a reação de beclin-1 e caspase-3 nas células foliculares, associada com acumulação de vacúolos autofágicos após a reabsorção completa do vitelo, é um passo crucial no gatilho da morte celular durante atresia folicular (Morais et al., 2012). Em peixes, estudos têm indicado que ambas apoptose e autofagia trabalham em conjunto e um papel duplo tem sido atribuído à autofagia durante a atresia folicular (Thomé et al., 2009; Morais et al., 2012) (Figura 4).

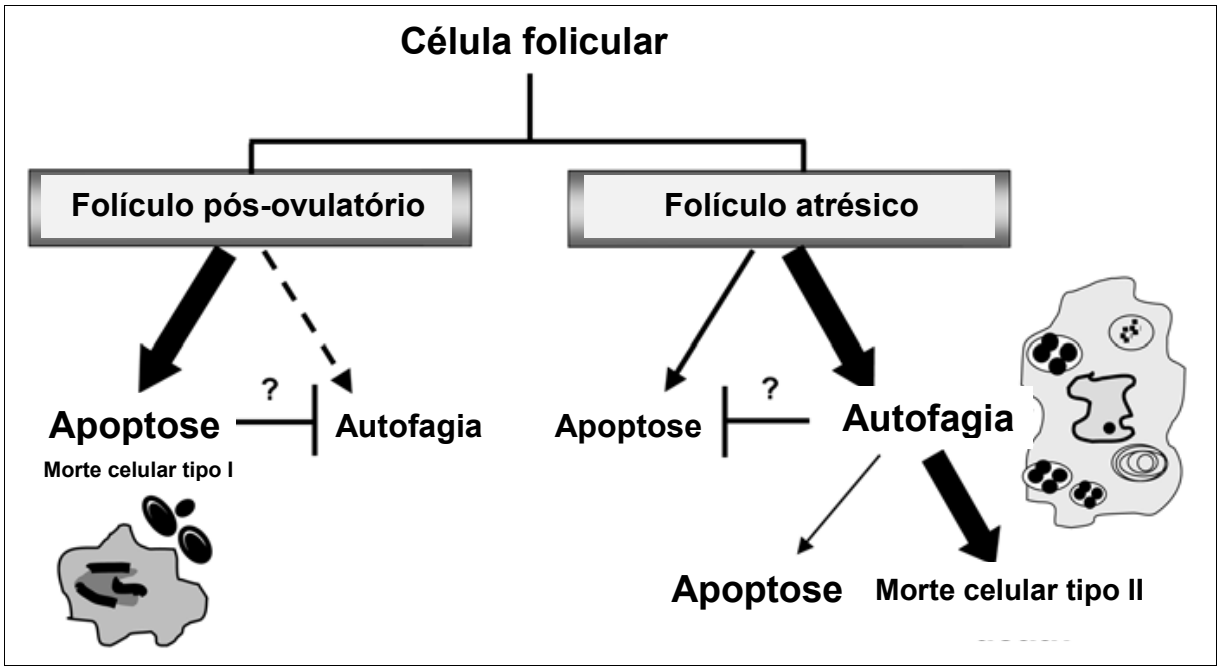

Figura 4. Esquema mostrando o destino das células foliculares em ovários de peixes ovíparos após a desova (Thomé et al., 2009).

Apesar de recentes contribuições sobre os processos de morte celular durante o desenvolvimento e funcionamento ovariano em vertebrados (Sundaresan et al., 2007; Choi et al., 2011; Matsuda et al., 2012; Morais et al., 2012), o conhecimento dos mecanismos envolvidos na remodelação ovariana pós-desova ainda é incipiente. Deste modo, o presente trabalho teve como principal objetivo avaliar a dinâmica de remodelação tecidual dos ovários da tilápia-do-nilo após a desova em cativeiro. Em um primeiro artigo científico, foi avaliada a dinâmica morfológica e quantitativa do crescimento folicular após desova, e no segundo artigo, o papel da apoptose e autofagia no crescimento e regressão folicular pós-desova em ovários de *O. niloticus*.

2- OBJETIVOS

2.1- OBJETIVO GERAL

Avaliar a dinâmica de remodelação tecidual dos ovários da tilápia-do-nilo (*O. niloticus*) após a desova em cativeiro.

2.2- OBJETIVOS ESPECÍFICOS

- Analisar a dinâmica histológica, ultraestrutural e quantitativa dos folículos ovarianos após a desova (Artigo científico I);

- Analisar, quantificar e comparar as características histológicas, ultraestruturais e imunohistoquímicas da morte celular durante a remodelação ovariana pós-desova (Artigo científico II).

3- MATERIAIS E MÉTODOS

3.1- AMOSTRAGEM

O experimento foi conduzido no Laboratório de Aquacultura da Escola de Veterinária da Universidade Federal de Minas Gerais (UFMG), sudeste do Brasil, durante os meses de novembro e dezembro de 2010. O projeto de pesquisa foi aprovado pelo Comitê de Ética em Experimentação Animal (CETEA) da UFMG. Para indução da reprodução de *O. niloticus*, 48 fêmeas e 16 machos adultos foram distribuídos em oito tanques de 1 m^3 (6 fêmeas para 2 machos/tanque), com aeração contínua por difusor de ar, temperatura ambiente da água entre 26 e 28 ºC e alimentados *ad libitum* duas vezes ao dia com ração comercial (32% proteína bruta). Após três dias de estocagem, as fêmeas foram inspecionadas na cavidade bucal para sinalização da desova, e daquelas que reproduziram, a prole foi retirada para prevenir o cuidado parental. Para assegurar que todos exemplares estivessem na mesma condição reprodutiva, 12 fêmeas imediatamente desovadas foram transferidas e mantidas em tanque de 5 m^3 com revestimento de geomembrana, aeração suplementar contínua por difusor de ar, aquecedores com termostatos para manutenção da temperatura e fotoperíodo de 12:12 luz:escuro. O sistema de cultivo também estava munido com tubo de drenagem central perfurado na parte inferior para facilitar remoção de resíduos em sistema de recirculação de água, onde cerca de 50% da água foi trocada duas vezes por semana por água de mesma temperatura. Os parâmetros físico-químicos da água foram monitorados semanalmente (temperatura: 29,5 ± 1,5 °C, oxigênio dissolvido: 6,70 ± 1,46 mg/L, pH: 7,68 ± 0,31, condutividade: 0,28 ± 0,05 mS/cm, sólidos dissolvidos totais: 0,16 ± 0,03 g/L, salinidade: 0,12 ± 0,02 ppt e turbidez: 1,71 ± 0,38). Os peixes foram alimentados *ad libitum* duas vezes ao dia com ração comercial (32% proteína bruta, 6-8 mm extrusada), e 30 minutos após a alimentação as sobras eram recolhidas. As fêmeas foram manejadas na ausência de machos

durante o experimento, evitando, desta forma, a influência de diversos fatores complexos de uma estimulação conespecífica.

Para analisar a remodelação ovariana pós-desova, três fêmeas foram coletadas nos seguintes tempos: imediatamente após a desova (0), 7 dias após a desova (+7), 14 dias após a desova (+14) e 21 dias após a desova (+21). Os peixes foram sacrificados por secção transversal da medula espinhal, de acordo com as normas estabelecidas pelo Colégio Brasileiro para Experimentação Animal (COBEA). De cada exemplar, foram obtidos o comprimento total (CT), peso corporal (PC) e gonadal (PG), e o índice gonadossomático (IGS = 100 PG/PC). Amostras seriais da região medial dos ovários de cada espécime foram coletadas para o emprego de diversas técnicas.

3.2- MICROSCOPIAS DE LUZ E ELETRÔNICA DE TRANSMISSÃO

Amostras de ovários de cada animal foram fixadas em líquido de Bouin por 24 horas, incluídas em parafina, seccionadas com 5 μm de espessura e coradas com hematoxilina-eosina, tricrômico de Gomori e PAS contra-coradas com hematoxilina.

Fragmentos de ovários foram fixados em solução de Karnovsky modificado (glutaraldeído 2,5% e paraformaldeído 2% em tampão fosfato 0,1M pH 7,3) durante 24h a 4ºC. Em seguida, os espécimes foram pós-fixados em tetróxido de ósmio 1% com ferrocianeto de potássio 1,5% por 2h e incluídos em resina Epon/Araldite. Os cortes ultrafinos foram contrastados com acetado de uranila e citrato de chumbo e examinados ao microscópio eletrônico de transmissão Tecnai G2-12 Spirit a 120 kV.

3.3- TUNEL IN SITU

Para identificação da fragmentação do DNA das células em apoptose, amostras do ovário de cada espécime foram fixadas em paraformoldeído 4% em tampão fosfato de sódio 0,1M em pH 7,3, incluídas em parafina, seccionadas com 5 μm de espessura e submetidas à

técnica de TUNEL *in situ* utilizando o kit da Calbiochem (QIA33) de acordo com o protocolo do fabricante. Antes da reação, os cortes foram lavados com tampão Tris-HCl 0,01 M pH 7,6 (TBS) e tratados com proteinase K 20 μg/ml em TBS por 20 min e água oxigenada 3% em TBS por 30 min para permeabilização e inativação de peroxidase endógena respectivamente. Em seguida, as secções foram incubadas com mistura da enzima terminal deoxynucleotides transferase (TdT) e deoxinucleotídeos conjugados com biotina em câmara úmida a 37ºC por 3h. Posteriormente, os cortes receberam solução de estreptavidina conjugada com peroxidase em câmara úmida a temperatura ambiente por 45 min. A reação da peroxidase foi revelada com diaminobenzidina (DAB) durante 8 min à temperatura ambiente. As lâminas foram contra-coradas com hematoxilina. O controle negativo foi realizado retirando TdT e deoxinucleotídeos.

3.4- IMUNOFLUORESCÊNCIA

Para avaliação de caspase 3 (anticorpo monoclonal de camundongo, sc-7272, Santa Cruz Biotechnology) na microscopia de fluorescência, amostras de ovário de cada espécime foram fixadas em paraformoldeído 4% em tampão fosfato de sódio 0,1M em pH 7,3, incluídas em parafina, seccionadas com 4-6 μm de espessura em lâminas silanizadas. Para reativação antigênica foi utilizado pré-tratamento com tampão citrato pH 6,0 a 95º por 30 min. Para bloqueio de reações inespecíficas e da peroxidase endógena foram utilizados albumina de soro bovino (BSA) 2% e água oxigenada 3%, respectivamente. As secções histológicas foram incubadas com anticorpo primário "overnight" a 4ºC, onde a diluição utilizada para caspase 3 foi de 1:100. Para a detecção de imunofluorescência foram utilizados anticorpos secundários Alexa 488 anti-coelho. Os controles negativos foram realizados omitindo o tratamento com o anticorpo primário. As secções foram avaliadas com a utilização de microscópio confocal Zeiss 510 Meta.

3.5- MORFOMETRIA

Em cortes histológicos transversais do ovário de cada espécime, o número de folículos em cada fase de desenvolvimento foi contado e a proporção relativa (%) de cada folículo foi obtida a partir do número total de folículos por corte. Para cada folículo ovariano, foi medido o diâmetro, do maior eixo longitudinal, de 50 folículos íntegros por período amostrado, utilizando régua micrométrica acoplada a ocular do microscópio de luz.

A área (μm²) dos folículos ovarianos íntegros e a altura (μm) das células foliculares de folículos maduros, FPO e FA também foi calculada, por período amostrado, com auxílio do software Motic Images Plus 2.0. A proporção relativa (%) de folículos contendo células apoptóticas marcados por TUNEL foi calculada para cada folículo ovariano. O índice apoptótico (I_A = 100 CA/CF, onde CA = células apoptóticas coradas por TUNEL and CF = todas as células foliculares) foi determinado para as células foliculares no FPO e FA. Os valores de proporção relativa de TUNEL, área dos folículos, altura das células foliculares e I_A foram calculados usando 40 folículos para cada estágio de desenvolvimento/regressão.

3.6- ANÁLISES ESTATÍSTICAS

Um teste G de aderência foi utilizado para verificar diferenças significativas entre as proporções relativas dos folículos por período amostral. Os valores de diâmetro dos folículos foram comparados utilizando teste Kruskal-Wallis seguido pelo teste de Dunn para determinar diferenças significativas entre as médias. Os dados de área dos folículos, altura das células foliculares e I_A mostraram distribuição normal, portanto para verificar diferenças significativas entre as médias destas variáveis foi utilizado o teste ANOVA seguido pelo teste de Tukey. Os valores do FPO foram analisados pelo teste t de Student. A correlação de Pearson foi utilizada para determinar o grau de associação entre o I_A e os parâmetros morfométricos. As análises estatísticas foram realizadas com o auxílio dos softwares BioEstat 5.3, Minitab 16.1 e GraphPad Prism 6.03, com o nível de significância $P \leq 0.05$.

4- RESULTADOS

4.1- ARTIGO 1: MORPHOLOGICAL AND QUANTITATIVE EVALUATION OF THE OVARIAN RECRUDESCENCE IN NILE TILAPIA (*OREOCHROMIS NILOTICUS*) AFTER SPAWNING IN CAPTIVITY

REVIEW

Morphological and Quantitative Evaluation of the Ovarian Recrudescence in Nile Tilapia (*Oreochromis niloticus*) After Spawning in Captivity

Rafael Magno Costa Melo,[1] Yuri Simões Martins,[1] Edgar de Alencar Teixeira,[2] Ronald Kennedy Luz,[2] Elizete Rizzo,[1] and Nilo Bazzoli[3]*

[1]*Departamento de Morfologia, Instituto de Ciências Biológicas, Universidade Federal de Minas Gerais, Belo Horizonte, Minas Gerais, Brazil*
[2]*Laboratório de Aquacultura, Escola de Veterinária, Universidade Federal de Minas Gerais, Belo Horizonte, Minas Gerais, Brazil*
[3]*Programa de Pós-graduação em Zoologia de Vertebrados, Pontifícia Universidade Católica de Minas Gerais, Belo Horizonte, Minas Gerais, Brazil*

ABSTRACT The Nile tilapia is one of the most important fish species for aquaculture worldwide. Understanding their reproductive biology is essential for improving their aquaculture methods. The morphological and quantitative dynamics of ovarian recrudescence of *Oreochromis niloticus* was studied for 21 days postspawning. To accomplish this, breeding females were kept in controlled conditions and ovarian samples were collected weekly for histological, ultrastructural and morphometric analyses. Ovarian follicle morphology revealed an intense synthesis activity of the follicular cells, which actively contributed to formation of the zona radiata and oocyte development following spawning. Recently spawned ovaries contained follicles at all developmental stages, but they were predominantly early primary growth (~42%) and full-grown follicles (~20%). Remnants of spawning, postovulatory follicle complexes represented approximately 5% of the former ovarian follicles immediately after spawning, and less than 1% after 7 days. Atretic follicles accounted for approximately 2% of the follicles studied during the period. The stock of primary growth follicles was stable during ovarian recrudescence, indicating their availability for continuous recruitment. Only the frequency of full-grown follicles significantly increased in the ovaries during recrudescence, representing approximately 35% of the follicles 21 days postspawning. The diameters of all follicles were significantly different between the periods analyzed. The ovaries' morphological characteristics, the maintenance of young follicles stocks and the gradual and significant increase in the proportion and diameter of full-grown follicles showed a rapid ovarian recovery and follicular growth of *O. niloticus*, in 21 days at 29.5°C, necessary for the next spawning. J. Morphol. 275:348–356, 2014.

KEY WORDS: fish ovary; reproduction; ovarian morphology; oocyte development; follicle complex; follicular growth

INTRODUCTION

The tilapias constitute one of the most important groups of fish for aquaculture worldwide. The Nile tilapia, *Oreochromis niloticus* (Linnaeus, 1758), is, by far, the most important species of cultivated tilapia, with an estimated production, in 2010, of 2.5 million tons and market value of more than $4 billion (FAO, 2012). Among the characteristics that make the tilapias attractive for aquaculture are excellent growth and reproduction in different environmental conditions, resistance to diseases and infections, and tolerance to stress induced by handling (Coward and Bromage, 2000; Little and Hulata, 2000).

An important reproductive aspect to tilapia culture is gonadal recrudescence after spawning (Gunasekera and Lam, 1997). Tilapias have breeding frequency variability even under controlled environmental conditions (Coward and Bromage, 1999). Spawns occur at 3–4 week intervals (Jalabert and Zohar, 1982; Tacon et al., 1996; Coward and Bromage, 2000). The interspawning interval (ISI) may be influenced by the size, age and fish lineage, stocking density, sex ratio, temperature, photoperiod, and nutritional status (Gunasekera et al., 1996; Ridha and Cruz, 1999; Little and Hulata, 2000; Campos-Mendoza et al., 2004). The frequency of spawning among tilapias can also be influenced by social interaction and audible and

*Correspondence to: Nilo Bazzoli, Programa de Pós-Graduação em Zoologia de Vertebrados, PUC Minas, Av. Dom José Gaspar, 500, postal address: 30535-610, Belo Horizonte, Minas Gerais, Brazil. E-mail: bazzoli@pucminas.br

Received 8 March 2013; Revised 30 August 2013;
Accepted 9 September 2013.

Published online 18 October 2013 in
Wiley Online Library (wileyonlinelibrary.com).
DOI 10.1002/jmor.20214

chemical stimuli of their conspecifics (Coward and Bromage, 2000).

Ovarian development in tilapias has been described by some authors (Babiker and Ibrahim, 1979; Tacon et al., 1996; Coward and Bromage, 1998) and has some similarities to that of many teleost fish (Tyler and Sumpter, 1996; Patiño and Sullivan, 2002; Lubzens et al., 2010). In most teleosts, folliculogenesis begins with proliferation and differentiation of primordial germ cells, produce distinct types of oogonia that are found in the germinal epithelium that borders the ovarian lamellae (Grier et al., 2009). The single A-undifferentiated oogonia divide by mitosis giving rise to single A-differentiated oogonia that proliferate to generate B-oogonia, forming germline cysts. Within the cysts, B-oogonia enter meiosis becoming oocytes (Quagio-Grassiotto et al., 2011). When folliculogenesis is completed, the ovarian follicle, comprising an oocyte and the encompassing follicle cells, is surrounded by a basement membrane and theca, resulting in the formation of a follicle complex (Grier, 2012). During follicular growth, there are two distinct stages: primary growth and secondary growth. Primary growth includes cytoplasmic and nuclear changes, including one and multiple nucleoli steps, in the oocytes as well as the rapid accumulation of cortical alveoli. Secondary growth is characterized by the rapid accumulation of yolk globules in ooplasm and large increase in the follicles diameter (Patiño and Sullivan, 2002; Grier et al., 2009; Lubzens et al., 2010). After spawning, a newly formed postovulatory follicle complex (POC), composed of a basement membrane that separates the follicular cells from theca, remains attached to the germinal epithelium (Grier, 2012). Atretic follicles also occur in fish ovaries. These are nonovulated ovarian follicles that are resorbed in a process called follicular atresia (Santos et al., 2005; Morais et al., 2012).

Despite the fact that *O. niloticus* is among the five economically most important species in aquaculture worldwide (FAO, 2012), low fecundity and asynchronous spawning cycles of female broodstock are significant restrictions for the commercial production of tilapias (Coward and Bromage, 2000; Little and Hulata, 2000). Hence, increasing the knowledge of the reproductive biology of the breeding females is of great importance to the improvement of tilapia cultivation. The aim of this study was to evaluate the morphological and quantitative dynamics of follicular growth during ovarian recrudescence in broodstock females of *O. niloticus* after spawning in captivity.

MATERIALS AND METHODS

Fish Stocking and Sampling

The study was conducted at the Aquaculture Laboratory of the School of Veterinary Medicine, Federal University of Minas Gerais (19°52′16.42″S 43°58′13.90″W), south-eastern Brazil, during the months of November and December of 2010. For reproduction of *Oreochromis niloticus* (Linnaeus, 1758), a breeding stock of adult females and males, previously kept under ordinary cultivation conditions, were distributed in 1 m^3 tanks, with the water temperature being between 26 and 28°C. The fish were fed ad libitum twice a day with commercial feed (32% crude protein). After 3 days of being stocked at a ratio of one male:three females, the oral cavity of spawned females was emptied of eggs to prevent further mouthbrooding. To ensure that all specimens were in the same reproductive condition, the twelve immediately spawned females were transferred and kept in a 5 m^3 tank with geomembrane liner, continuous supplementary aeration by an air diffuser, heaters with thermostatic control to maintain the temperature and photoperiod of 12 h:12 h light:dark (L:D). The physicochemical parameters of the water were monitored weekly (temperature: 29.5 ± 1.5°C, dissolved oxygen: 6.70 ± 1.46 mg l^{-1}, pH: 7.68 ± 0.31, conductivity: 0.28 ± 0.05 mS cm^{-1}, total dissolved solids: 0:16 ± 0.03 g l^{-1}, salinity: 0.12 ± 0.02 ppt, and turbidity: 1.71 ± 0.38 NTU). The fish were fed ad libitum twice a day with commercial feed (32% crude protein), and the remainder was collected 30 min after feeding. Females were handled separately from males during the study, to avoid conspecific stimulation.

To analyze the ovarian recrudescence, three females were killed weekly by transverse section of the cervical medulla, in accordance with the ethics principles established by the Brazilian College for Animal Experimentation, during the study period: immediately spawned (0), 7 days after spawning (+7), 14 days after spawning (+14), and 21 days after spawning (+21). From each female, total (TL) length, body (BW), and gonad (GW) weights were obtained, and also the gonadosomatic index (GSI = 100 GW BW^{-1}): 34.89 ± 2.64 cm TL; 661.14 ± 161.83 g BW; 12.96 ± 6.34 g GW; 1.93 ± 0.76 GSI. Samples of the medial region of the ovaries of each specimen were collected for morphological and quantitative analyses.

Light Microscopy

Samples of ovaries (n = 12 specimens) were fixed in Bouin's fluid for 24 h at room temperature and then embedded in paraffin. Transverse histological sections of 3–5 μm thickness were mounted in glass slides and stained with hematoxylin–eosin, Gomori's trichrome, and periodic acid-Schiff (PAS) counter stained with hematoxylin.

Transmission Electron Microscopy

For the transmission electron microscopy ovarian samples (n = 12 specimens) were fixed in modified Karnovsky solution (2.5% glutaraldehyde and 2% paraformaldehyde) buffered in 0.1 mol l^{-1} phosphate (pH 7.3) for 12 h at 4°C. The samples were postfixed in 1% osmium tetroxide with 1.5% potassium ferrocyanide for 2 h, and then embedded in Epon/Araldite plastic resin. Ultrathin sections were cut with a diamond knife and stained with uranyl acetate and lead citrate, and examined using a Tecnai G2-12 Spirit transmission electron microscope at 120 kV.

Morphometric and Statistical Analyses

The numbers of all ovarian follicles were counted in a transverse histological section, with preserved tunica albuginea, of each specimen. The relative proportion (%) of each follicle was obtained from the total number of follicles per section. For each ovarian follicle, the diameter of the largest longitudinal axis was measured of 50 intact follicles per sampling period, using a micrometric ruler attached to an ocular light microscope. Due to the irregular shape, the diameter of POCs and atretic follicles was not measured. Values are expressed as mean ±SD per sampling period.

A G-test of independence was used to verify significant differences between the relative proportions of ovarian follicles per sampling period and between sampling periods. Percentage

values followed by different superscript letters are significantly different ($P \leq 0.05$). The averages of the ovarian follicle diameters were compared using Kruskal-Wallis (H) test followed by Dunn's *post hoc* test to determine significant differences among the mean values. Statistical analyses were performed with the aid of the BioEstat 5.3 and GraphPad Prism 5.0 softwares, with significance level of $P \leq 0.05$.

RESULTS

Histological and Ultrastructural Observations

Ovaries of *Oreochromis niloticus* are paired organs, secular structure, and unite at the caudal end to form the common gonoduct, which communicates with the urogenital papilla (Fig. 1A). Histologically, the ovaries are surrounded by a thick tunica albuginea, comprised of connective tissue, collagen fibers, nerves, and blood vessels, which sends septa into the organ forming ovarian lamellae. The epithelial covering of the lamellae is a germinal epithelium where germ cells and follicles are found (Fig. 1B,C). Different types of oogonia (A-undifferentiated, A-differentiated, and B-oogonia) were observed, with a discontinuous distribution along the germinal epithelium, in all analyzed ovaries (Figs. 1B, 2A inset, 3A inset). Ovarian follicles at different stages of development were quantified during the study period: early and late primary growth, early secondary growth and full-grown follicles, besides POCs and atretic follicles. The main histological and ultrastructural characteristics of the follicles during *O. niloticus* ovarian recrudescence are summarized in Table 1 and in Figures 1–3.

Ovarian Recrudescence Morphometry

Immediately after spawning, *O. niloticus* ovaries have a significantly higher proportion (%) of early primary growth follicles (42.2 ± 15.9^{a}), followed by full grown (20.3 ± 10.9^{b}), late primary growth (19.2 ± 6.0^{b}), and early secondary growth (11.1 ± 5.0^{b}) follicles, and lower proportion of POCs (4.6 ± 1.8^{c}) and atretic (2.6 ± 0.9^{c}) follicles (G-test = 61.457, $P < 0.0001$; Fig. 1).

Seven days postspawning, ovaries exhibited significantly higher proportion of early primary growth (36.8 ± 6.4^{a}) and full-grown ($23.9 \pm 5.2^{a,b}$) follicles, followed by late primary growth (21.5 ± 6.3^{b}) and early secondary growth (14.5 ± 1.2^{b}) follicles, besides atretic follicles (2.5 ± 0.8^{c}) and POCs (0.8 ± 0.2^{c}; G-test = 68.175, $P < 0.0001$; Fig. 2).

Ovaries, 14 days after spawning, maintained the predominance of early primary growth (37.9 ± 6.3^{a}) and full-grown ($25.2 \pm 2.7^{a,b}$) follicles, followed by late primary growth (18.8 ± 3.4^{b}) and early secondary growth (15.8 ± 3.2^{b}) follicles, besides atretic follicles (2.3 ± 1.1^{c}; G-test = 73.062, $P < 0.0001$; Fig. 2).

After 21 days of ovarian recrudescence, there was predominance of full grown (35.1 ± 15.4^{a}), early (28.9 ± 11.3^{a}) and late primary growth ($21.1 \pm 7.7^{a,b}$) follicles, followed by early secondary growth (12.5 ± 2.6^{b}) and atretic (2.4 ± 1.3^{c}) follicles (G-test = 41.036, $P < 0.0001$; Fig. 3).

During the ovarian recrudescence of *O. niloticus*, only the proportion of full-grown follicles (0 and +21: G-test = 4.002, $P = 0.0454$) had a significant difference between the periods analyzed (Fig. 4). The diameters of the early ($H = 18.162$, $P = 0.0004$) and late ($H = 53.311$, $P < 0.0001$) primary growth, early secondary growth ($H = 25.974$, $P < 0.0001$) and full-grown ($H = 90.844$, $P < 0.0001$) follicles showed significant differences between the periods analyzed (Table 2).

DISCUSSION

In this study, females of *Oreochromis niloticus* were deprived of conspecific contact, and other factors such as temperature and water quality, photoperiod, size, and feed quality were strictly controlled. The values of the water physicochemical parameters and the culture conditions were in the acceptable range for gonadal development and reproduction of the Nile tilapia (Gunasekera et al., 1996; Ridha and Cruz, 1999; Little and Hulata, 2000; Lapeyre et al., 2010). The spawned females also had their offspring taken away, to prevent parental care. This type of handling usually accelerates the recrudescence of ovarian follicles in mouthbrooding tilapias (Tacon et al., 1996; Coward and Bromage, 2000).

Immediately spawned ovaries of *O. niloticus* contained follicles at all developmental stages, but early primary growth follicles were predominant. The present study suggests that a batch of full-grown follicles was already present when spawning occurred, due to presence of 20% of these follicles in the recently spawned ovaries. This percentage is similar to the one found in recently spawned females of *Tilapia zillii* (Coward and Bromage, 1998). Remnants of spawning, POCs, occupied 5% of the ovaries immediately after the spawning of *O. niloticus*, and after 7 days, the relative proportion has not reached to 1%. In *T. zillii*, involution of the POCs occurred just 3 days after spawning (Coward and Bromage, 1998). Atretic follicles comprised approximately 2% of the ovaries of *O. niloticus* during the study period, as observed in ovaries of *T. zillii* through the reproductive cycle, where atretic follicles comprised nearly 2% of the ovaries (Coward and Bromage, 1998). Due to the small variation in the relative proportion of atretic follicles during study period, it is suggested that the follicular atresia observed in *O. niloticus* was physiological under the cultive conditions used.

Our histological and ultrastructural data demonstrated that, during ovarian recrudescence of *O. niloticus*, features of the postovulatory and atretic

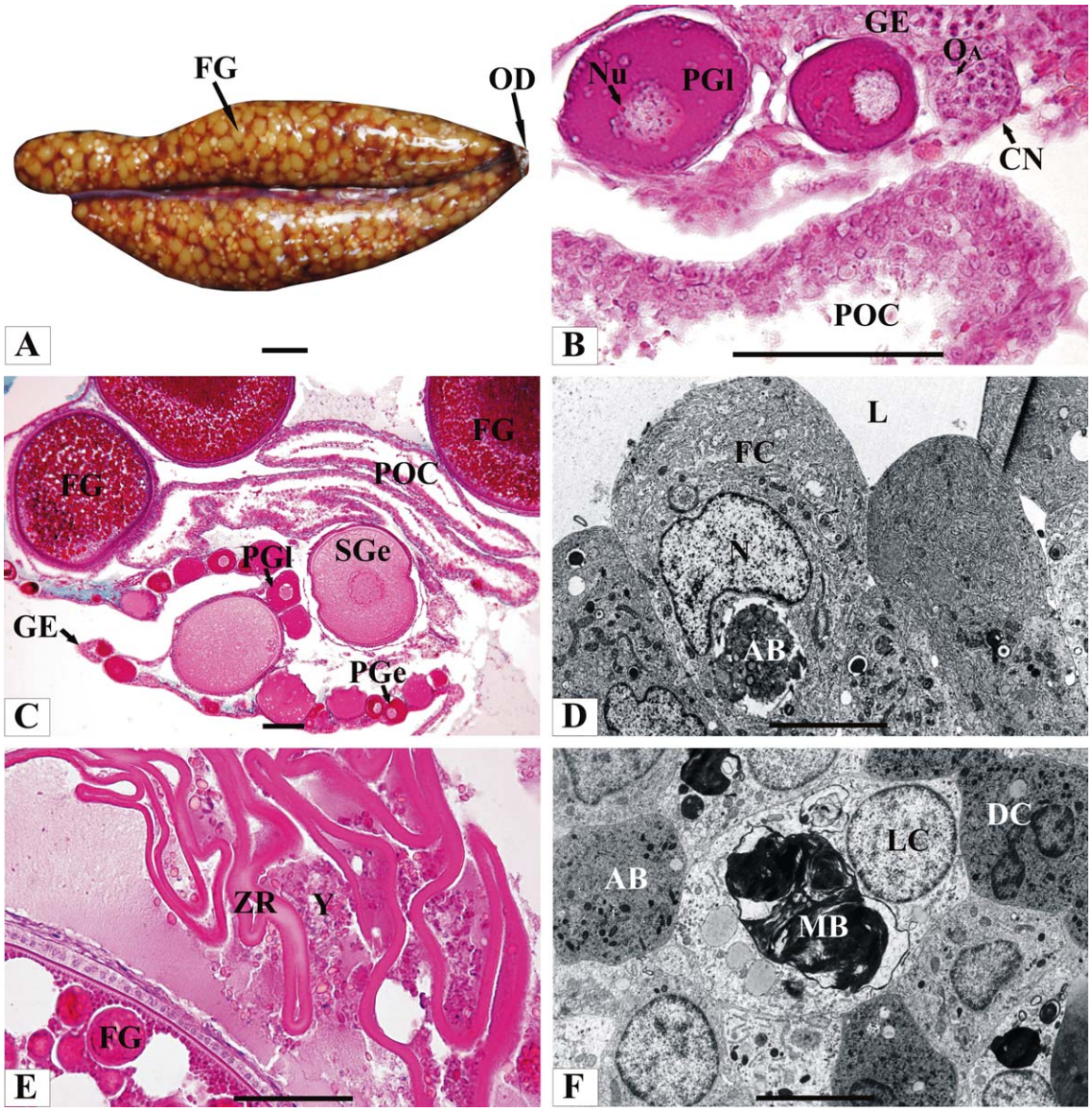

Fig. 1. Macroscopic characteristics (**A**), histological sections stained with hematoxylin-eosin (**B** and **E**), and Gomori trichrome (**C**), and transmission electron microscopy (**D** and **F**) of the ovaries, immediately after spawning, of *Oreochromis niloticus*. A: Sacciform ovaries after spawning, presenting hemorrhagic areas and full-grown follicles visible macroscopically. B: Partially spawned ovary illustrating the germinal epithelium and a cell nest contained germ cells. Two primary growth follicles are adjacent to a POC. C: Partially spawned ovary with POC, early and late primary growth, early secondary growth, and full-grown follicles. D: Ultrastructure of POC showing hypertrophied follicular cells with apoptotic body and adjacent follicular lumen. E: Atretic follicle with intact zona radiata and liquefied yolk. F: Ultrastructure of atretic follicle showing electron-lucid and electron-dense cells, multilamellar bodies, and apoptotic body. Full-grown follicle (FG), common ovarian duct (OD), germinal epithelium (GE), cell nest (CN), a-differentiated oogonia (OA), late primary growth follicle (PGl), nucleoli (Nu), postovulatory follicle complex (POC), early primary growth follicle (PGe), early secondary growth follicle (SGe), follicular cells (FC), follicular lumen (L), nucleus (N), apoptotic body (AB), zona radiata (ZR), yolk (Y), electron-lucid cells (LC), electron-dense cells (DC), multilamellar bodies (MB). Scale bars: A (0.5 cm); B, C, and E (200 μm); D and F (5 μm). [Color figure can be viewed in the online issue, which is available at wileyonlinelibrary.com.]

follicles, including evidence of apoptotic cell death, were similar to those of other teleosts (Santos et al., 2005; Thomé et al., 2009). However, some atretic follicles presented an apparently intact zona radiata, unlike those atretic follicles of some neotropical teleosts, in which the zona radiata is totally fragmented and reabsorbed in the early stages of follicular atresia (Santos et al., 2008; Morais et al., 2012).

During ovarian recrudescence of *O. niloticus*, follicles were found in all developmental stages, indicating asynchronous development of the ovaries, as reported for females of Tilapiine (Coward and Bromage, 2000). The distribution of ovarian

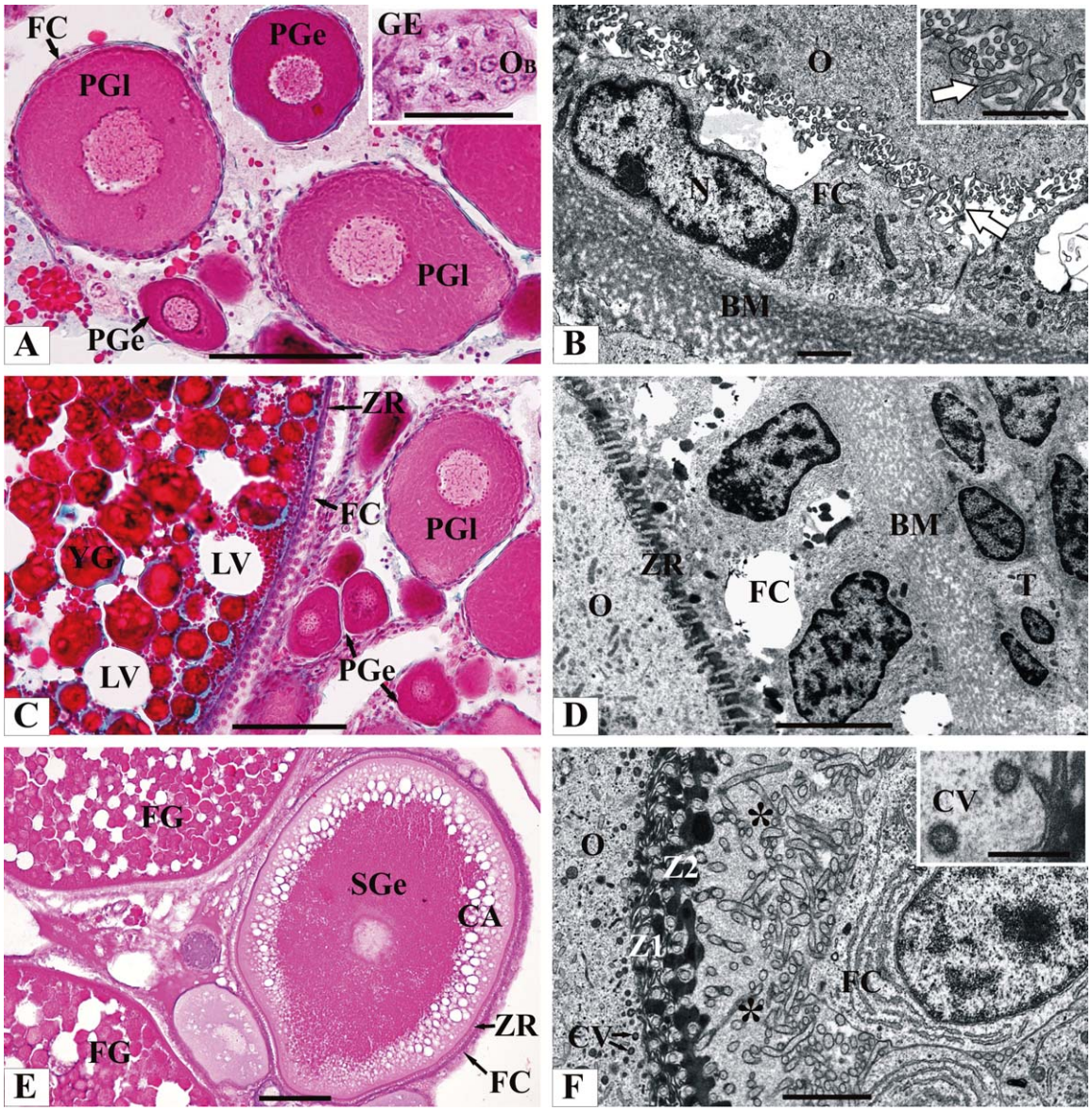

Fig. 2. Histological sections stained with Gomori trichrome (**A** and **C**), hematoxylin-eosin (inset A) and PAS-hematoxylin (**E**), and transmission electron microscopy (**B**, **D**, and **F**) of the ovaries, 7 and 14 days after spawning, of *Oreochromis niloticus*. A: Ovary with nest of B-oogonia in the germinal epithelium (inset), early and late primary growth follicles with squamous follicular cells from an ovary 7 days postspawning. B: Ultrastructure of early primary growth follicle showing intense contact between the cytoplasmic processes of follicular cells and oocyte microvilli (inset). C: Early and late primary growth follicles, and a full-grown follicle with conspicuous lipid vesicles, rounded yolk globules, thin zona radiata, and cuboidal follicular cells from an ovary 14 days postspawning. D: Ultrastructure of late primary growth follicle having a thin zona radiata in formation, squamous follicular cells, basal membrane, and connective theca. E: Full-grown follicles adjacent to the early secondary growth follicle with cortical alveoli in the peripheral ooplasm, thin zona radiata, and cuboidal follicular cells from an ovary 14 days postspawning. F: Ultrastructure of early secondary growth follicle showing deposition of eletron-dense material, by follicular cells, to form the outer layer of the zona radiata. Coated vesicles were frequently observed in peripheral ooplasma (inset). Early primary growth follicle (PGe), late primary growth follicle (PGl), follicular cells (FC), b-oogonia (OB), germinal epithelium (GE), basal membrane (BM), nucleus (N), interaction microvilli oocyte-processes follicular cells (white arrow), oocyte (O), yolk globules (YG), lipidic vesicles (LV), zona radiata (ZR), theca (T), early secondary growth follicle (SGe), full-grown follicle (FG), cortical alveoli (CA), inner zona radiata (Z1), outer zona radiata (Z2), eletron-dense material (asterisk), coated vesicles (CV). Scale bars: A, C, and E (100 μm); A inset (300 μm); B (1 μm); B inset (0.5 μm); D (5 μm); F (2 μm); F inset (0.5 μm). [Color figure can be viewed in the online issue, which is available at wileyonlinelibrary.com.]

follicles also showed great variability among the specimens. Studies report that the dynamics of ovarian development are highly variable among *O. niloticus* females, as shown by the extensive variation in the ISI (Jalabert and Zohar, 1982; Tacon et al., 1996; Gunasekera and Lam, 1997). This variability in ovarian development may result from individual physiological responses to a variety of

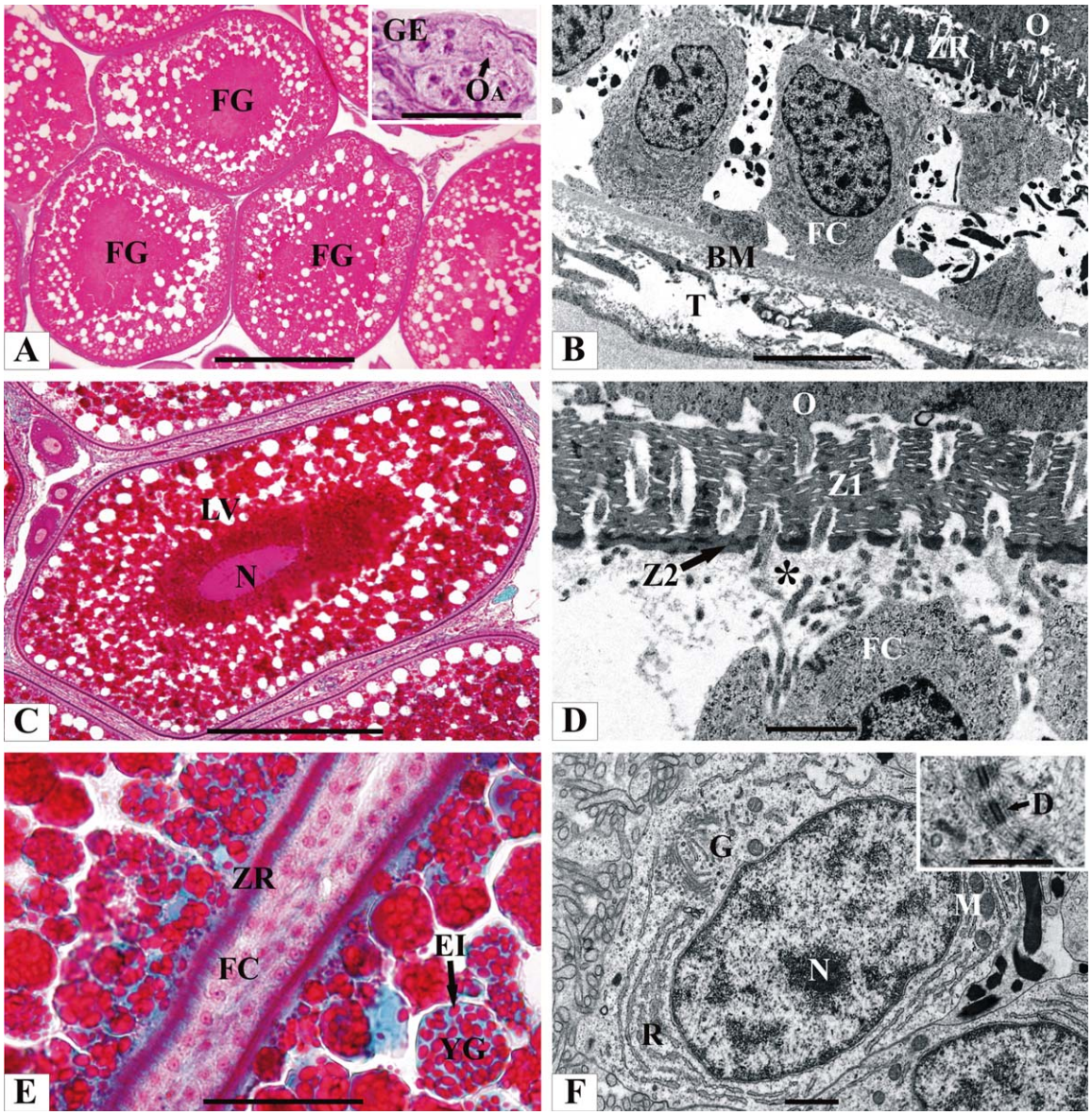

Fig. 3. Histological sections stained with hematoxylin-eosin (**A**, inset A), Gomori trichrome (**C** and **E**), and transmission electron microscopy (**B**, **D**, and **F**) of the ovaries, 21 days after spawning, of *Oreochromis niloticus*. A: Ovary in advanced maturation showing single oogonia in the germinal epithelium (inset) and predominance of full-grown follicles. B: Ultrastructure of full-grown follicle with thin zona radiata, cuboidal follicular cells, basal membrane and theca with fibroblast-like cells. C: Full-grown follicle with elliptical shape showing numerous lipidic vesicles. D: Ultrastructure of full-grown follicle presenting the inner and outer zona radiata and deposition of eletron-dense material by follicular cells. E: Full-grown follicles with spherical yolk globules with ellipsoid inclusions, thin zona radiata, and cuboidal follicular cells. F: Ultrastructure of a follicular cell showing cytoplasm with synthesis organelles. Follicular cells are joined by intercellular junctions, mainly desmosomes (inset). Full-grown follicles (FG), germinal epithelium (GE), a-undifferentiated oogonia (OA), oocyte (O), zona radiata (ZR), follicular cells (FC), basal membrane (BM), theca (T), nucleus (N), lipidic vesicles (LV), inner zona radiata (Z1), outer zona radiata (Z2), eletron-dense material (asterisk), yolk globules (YG), ellipsoid inclusions (EI), Golgi apparatus (G), rough endoplasmic reticulum (R), mitochondria (M), desmosomes (D). Scale bars: A (50 μm); A inset (300 μm); B (5 μm); C (100 μm); D and F (1 μm); E (200 μm); F inset (0.5 μm). [Color figure can be viewed in the online issue, which is available at wileyonlinelibrary.com.]

factors (Coward and Bromage, 2000). Despite follicle variability, females of *O. niloticus* maintained a stable stock of primary growth follicles during study period, and scattered nests of oogonia were also present in all analyzed ovaries. This suggests that stocks of oogonia and young follicles are constantly available for recruitment, an especially important feature for tilapias, which have multiple spawning with varying reproductive cycles (Jalabert and Zohar, 1982; Coward and Bromage, 2000).

During the follicular growth of *O. niloticus*, follicular cells are squamous during primary growth and cuboidal during secondary growth. This fact

TABLE 1. Histological and ultrastructural characteristics of the follicle complex, contained early (PGe) and late (PGl) primary growth, early secondary growth (SGe) and full-grown (FG) follicles, besides postovulatory follicle complex (POC) and atretic follicle (AF) of Oreochromis niloticus during ovarian recrudescence

Follicles	Morphology
Oogonias	Small rounded cell, with prominent nucleus and a single nucleolus, that forms nests in which originate ovarian follicles in the germinal epithelium (Figs. 1B, 2A -inset, 3A -inset).
PGe	Possess a central vesicular nucleus, with one nucleolus and "nuages" in the perinucleolar region, and intensely basophilic cytoplasm. The follicle complex is formed by squamous follicular cells, basal membrane and developing theca (Fig. 2A, B). Cytoplasmic projections of follicular cells and the oocyte microvilli are in contact intensively (Fig. 2B -inset).
PGl	Presents vesicular nucleus with several nucleoli close to the nuclear envelope, finely granular and less basophilic cytoplasm. The surrounding layers are a thin zona radiata, squamous follicular cells, thin basal membrane and theca. The formation of the zona radiata starts with the deposition of electron-dense material on its outer layer (Fig. 2C, D).
SGe	The nucleus is central and several nucleoli remain close to the nuclear envelope, the cytoplasmic basophilia decreases, and the cortical alveoli are located in the periphery of the ooplasm. The cuboidal follicular cells present intense synthesis activity and the zona radiata has two layers: an electron-lucid inner and an electron-dense outer (Fig. 2E, F). The oocyte starts uptake of vitellogenin, and coated vesicles are observed in the oocyte peripheral ooplasm (Fig. 2F -inset).
FG	Presents ovoid or elliptical form, central or eccentric nucleus, ooplasm filled with spherical yolk globules with ellipsoidal acidophilic inclusions, small cortical alveoli and conspicuous lipid vesicles. The zona radiata has a more developed electron-lucid fibrous inner layer with simple pore channels, and a thin electron-dense outer layer. The cuboidal follicular cells present evident synthesis machinery, and the theca has cells similar to fibroblasts (Fig. 3).
POC	Has hypertrophied follicular cells, thin basal membrane and theca, and wide lumen (Fig. 1C, D).
AF	Presents yolk liquefaction and reabsorption by the follicular cells and zona radiata PAS+ relatively intact (Fig. 1E, F).

may be related to the increase of the steroidogenic function of the follicular cells and theca during oocyte secondary growth (Kagawa et al., 1982; Tyler and Sumpter, 1996; Patiño and Sullivan, 2002). In fact, in this study, the follicle's ultrastructure revealed that the follicular cells showed intense synthesis activity and constant interaction with the oocyte during ovarian recrudescence, and actively participated in the zona radiata formation. In the process of oocyte growth, the vitellogenins, primarily synthesized in the liver (Babin et al., 2007), pass from the bloodstream to the theca capillaries and follow into the follicular cells, reaching the oocyte's surface, and through the zona radiata pore channels, are incorporated into the ooplasm (Lubzens et al., 2010). In *O. niloticus*, the zona radiata presented two layers: a thin external layer and a thick internal layer that appears to be fibrous, with simple pore channels. Histological data also showed two layers in the zona radiata in cichlids *Cichla kelberi* and *T. zillii* (Coward and Bromage, 1998; Martins et al., 2010). The conspicuous coated vesicles observed in the peripheral ooplasm of the Nile tilapia can play the role of sequester vitellogenins and other substances from the follicular cells, through micropinocytosis mediated by specific receptors (Wallace and Selman, 1990).

The ovaries of *O. niloticus* showed a predominance of full-grown follicles, which comprised approximately 35% of the ovaries, 21 days after spawning, period which the follicles also reached the largest diameter. In *T. zillii*, full-grown follicles predominated on the 8th day, occupying approximately 70% of the ovaries (Coward and Bromage, 1998). These differences in the ovarian development between Tilapiine species may be related to the different reproductive strategies adopted by the species, since *T. zillii* spawns on the substrate, has a higher batch fecundity, smaller eggs, and a shorter reproductive cycle than the mouthbrooding species, such as *O. niloticus* (Coward and Bromage, 1999, 2000).

When compared to other teleosts, it can be stated that the Nile tilapia has large-sized mature follicles, a characteristic usually associated with low fecundity and the expression of parental care

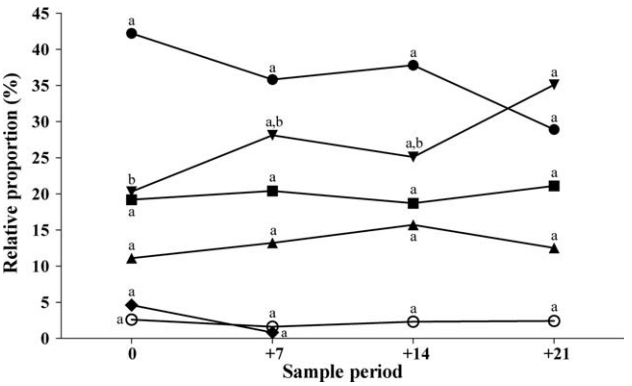

Fig. 4. Relative proportion of early (•) and late primary growth (■), early secondary growth (▲), full-grown (▼), postovulatory complex (◆), and atretic (○) follicles of *Oreochromis niloticus* during ovarian recrudescence (Number of total follicles: $n^0 = 953$, $n^{+7} = 702$, $n^{+14} = 492$, $n^{+21} = 481$). Percentage values followed by different superscript letters horizontally are significantly different ($P \leq 0.05$) by G-test of independence.

TABLE 2. Mean values (n = 50) of diameter ± S.D. of early (PGe) and late (PGl) primary growth, early secondary growth (SGe) and full-grown (FG) follicles of Oreochromis niloticus during ovarian recrudescence

	Follicles diameter (μm)			
Sample period	PGe	PGl	SGe	FG
0	45.50 ± 12.08[c]	111.74 ± 24.36[c]	338.16 ± 81.91[b]	832.89 ± 198.30[c]
+7	53.95 ± 15.98[a,b]	134.12 ± 24.36[b]	416.88 ± 77.10[a]	1233.70 ± 157.35[b]
+14	46.27 ± 12.67[b,c]	136.32 ± 21.65[a,b]	411.43 ± 79.03[a]	1298.11 ± 411.74[b]
+21	56.53 ± 15.62[a]	151.47 ± 21.45[a]	448.18 ± 101.99[a]	1442.16 ± 231.59[a]

Mean values followed by different superscript letters vertically are significantly different ($P \leq 0.05$) by Dunn's *post hoc* test.

(Melo et al., 2011). The ovoid shape of the *O. niloticus* full-grown follicles seems to be a common feature among tilapias (Coward and Bromage, 1998; Campos-Mendoza et al., 2004), and spherical yolk globules filled with ellipsoidal acidophilic inclusions were also observed in *C. kelberi* (Normando et al., 2009). Various lipid vesicles were observed in the full-grown oocytes of *O. niloticus*. These vesicles, usually observed in Perciformes fish, consist of neutral lipids and are rich in monounsaturated fatty acids, which act as metabolic energy reserves (Patiño and Sullivan, 2002; Martins et al., 2010).

In all ovarian follicles analyzed in *O. niloticus*, the significant increase in the diameter and the intense synthesis activity of the follicular cells, with secretion directed to the oocyte, revealed a rapid follicular growth during the ovarian recrudescence period. Similarly, the gradual and significant increase in the diameter of full-grown follicles indicates a positive relationship between the ISI period and egg size in the Nile tilapia. This relationship is probably due to the greater amount of time available for the follicles sequester vitellogenin from the bloodstream, resulting in larger-size follicles (Campos-Mendoza et al., 2004).

We conclude that, during *O. niloticus* ovarian recrudescence, the ovaries' morphological characteristics, the maintenance of young follicle stocks, and the gradual and significant increase in the proportion and diameter of full-grown follicles showed a rapid ovarian recovery and follicular growth, in 21 days at 29.5°C, to allow for the next spawning.

ACKNOWLEDGMENTS

The authors wish to thank the technicians at the Laboratory of Aquaculture (LAQUA) of the Federal University of Minas Gerais (UFMG) for their assistance in handling of the fishes; the technicians at the Microscopy Center of the UFMG for preparation of the biological material to the electron microscope; to Brazilian institutions CAPES (scholarship), CNPq, and FAPEMIG for financial support; and two anonymous referees for the review and improve of the manuscript.

LITERATURE CITED

Babiker MM, Ibrahim H. 1979. Studies on the biology of reproduction in the cichlid *Tilapia nilotica* (L.): Gonadal maturation and fecundity. J Fish Biol 14:437–448.

Babin PJ, Carnevali O, Lubzens E, Schneider WJ. 2007. Molecular aspects of oocyte vitellogenesis in fish. In: Babin PJ, Cerdà J, Lubzens E, editors. The Fish Oocyte: From Basic Studies to Biotechnological Applications. Dordrecht: Springer. pp 39–76.

Campos-Mendoza A, McAndrew BJ, Coward K, Bromage NR. 2004. Reproductive response of Nile tilapia (*Oreochromis niloticus*) to photoperiod manipulation; effects on spawning periodicity, fecundity and egg size. Aquaculture 231:299–313.

Coward K, Bromage NR. 1998. Histological classification of oocyte growth and the dynamics of ovarian recrudescence in *Tilapia zillii*. J Fish Biol 53:285–302.

Coward K, Bromage NR. 1999. Spawning periodicity, fecundity and egg size in laboratory-held stocks of a substrate-spawning tilapiine, *Tilapia zillii* (Gervais). Aquaculture 171: 251–267.

Coward K, Bromage NR. 2000. Reproductive physiology of female tilapia broodstock. Rev Fish Biol Fish 10:1–25.

Food and Agriculture Organization of the United Nations (FAO). 2012. Cultured Aquatic Species Information Programme: *Oreochromis niloticus* (Linnaeus, 1758). Available at: http://www.fao.org/fishery/culturedspecies/Oreochromis_niloticus/en. Accessed on June 9, 2012.

Grier HJ. 2012. Development of the follicle complex and oocyte staging in red drum, *Sciaenops ocellatus* Linnaeus, 1776 (Perciformes, Sciaenidae). J Morphol 273:801–829.

Grier HJ, Uribe AMC, Patiño R. 2009. The ovary, folliculogenesis, and oogenesis in teleosts. In: Jamieson BGM, editor. Reproductive Biology and Phylogeny of Fishes (Agnathans and Neotelestomi), Vol. 8A. Enfield, New Hampshire: Science Publishers. pp 25–84.

Gunasekera RM, Lam TJ. 1997. Influence of dietary protein level on ovarian recrudescence in Nile tilapia, *Oreochromis niloticus* (L.). Aquaculture 149:57–69.

Gunasekera RM, Shim KF, Lam TJ. 1996. Effect of dietary protein level on spawning performance and amino acid composition of eggs of Nile tilapia, *Oreochromis niloticus*. Aquaculture 146:121–134.

Jalabert B, Zohar Y. 1982. Reproductive physiology in cichlid fishes, with particular reference to *Tilapia* and *Soratherodon*. In: Pullin RSV, Lowe-McConnell RH, editors. The Biology and Culture of Tilapias. Manila: International Center for Living Aquatic Resources Management. pp 129–140.

Kagawa H, Young G, Adachi A, Nagahama Y. 1982. Estradiol-17β production in amago salmon (*Oncorhynchus rhodurus*) ovarian follicles: Roles of the thecal and granulosa cells. Gen Comp Endocrinol 47:440–448.

Lapeyre BA, Muller-Belecke A, Horstgen-Schwark G. 2010. Increased spawning activity of female Nile tilapia (*Oreochromis niloticus*) (L.) after stocking density and photoperiod manipulation. Aquac Res 41:561–567.

Little DC, Hulata G. 2000. Strategies for tilapia seed production. In: Beveridge MCM, McAndrew BJ, editors. Tilapias:

Biology and Exploitation. Great Britain: Kluwer Academic Publishing. pp 267–326.
Lubzens E, Young G, Bobe J, Cerdà J. 2010. Oogenesis in teleosts: How fish eggs are formed. Gen Comp Endocrinol 165: 367–389.
Martins YS, Moura DF, Santos GB, Rizzo E, Bazzoli N. 2010. Comparative folliculogenesis and spermatogenesis of four teleost fish from a reservoir in south-eastern Brazil. Acta Zool 91:466–473.
Melo RMC, Arantes FP, Sato Y, Santos JE, Rizzo E, Bazzoli N. 2011. Comparative morphology of the gonadal structure related to reproductive strategies in six species of neotropical catfishes (Teleostei: Siluriformes). J Morphol 272:525–535.
Morais RDVS, Thomé RG, Lemos FS, Bazzoli N, Rizzo E. 2012. Autophagy and apoptosis interplay during follicular atresia in fish ovary: A morphological and immunocytochemical study. Cell Tissue Res 347:467–478.
Normando FT, Arantes FP, Luz RK, Thomé RG, Rizzo E, Sato Y, Bazzoli N. 2009. Reproduction and fecundity of tucunaré, *Cichla kelberi* (Perciformes: Cichlidae), an exotic species in Três Marias Reservoir, Southeastern Brazil. J Appl Ichthyol 25:299–305.
Patiño R, Sullivan CV. 2002. Ovarian follicle growth, maturation, and ovulation in teleost fish. Fish Physiol Biochem 26: 57–70.
Quagio-Grassiotto I, Grier HG, Mazzoni TS, Nóbrega RH, Arruda AJP. 2011. Activity of the ovarian germinal epithelium in the freshwater catfish, *Pimelodus maculatus* (Teleostei: Ostariophysi: Siluriformes): Germline cysts, follicle formation and oocyte development. J Morphol 272:1290–1306.
Ridha MT, Cruz EM. 1999. Effect of different broodstock densities on the reproductive performance of Nile tilapia, *Oreochromis niloticus* (L.), in a recycling system. Aquac Res 30:203–210.
Santos HB, Rizzo E, Bazzoli N, Sato Y, Moro L. 2005. Ovarian regression and apoptosis in the South American teleost *Leporinus taeniatus* Lütken (Characiformes, Anostomidae) from the São Francisco Basin. J Fish Biol 67:1446–1459.
Santos HB, Thomé RG, Arantes FP, Sato Y, Bazzoli N, Rizzo E. 2008. Ovarian follicular atresia is mediated by heterophagy, autophagy, and apoptosis in *Prochilodus argenteus* and *Leporinus taeniatus* (Teleost: Characiformes). Theriogenology 70: 1449–1460.
Tacon P, Ndiaye P, Cauty C, Le Menn F, Jalabert B. 1996. Relationships between the expression of maternal behaviour and ovarian development in the mouthbrooding cichlid fish *Oreochromis niloticus*. Aquaculture 146:261–275.
Thomé RG, Santos HB, Arantes FP, Domingos FFT, Bazzoli N, Rizzo E. 2009. Dual roles for autophagy during follicular atresia in fish ovary. Autophagy 5:117–119.
Tyler CR, Sumpter JP. 1996. Oocyte growth and development in teleosts. Rev Fish Biol Fish 6:287–318.
Wallace RA, Selman K. 1990. Ultrastructural aspects of oogenesis and oocyte growth in fish and amphibians. J Electron Microsc Tech 16:175–201.

4.2- ARTIGO 2: ROLE OF APOPTOSIS, AUTOPHAGY AND CASPASE-3 DURING POST-SPAWNING OVARIAN REMODELING IN *OREOCHROMIS NILOTICUS*

Journal of Molecular Histology

Role of apoptosis, autophagy and caspase-3 during post-spawning ovarian remodeling in Oreochromis niloticus

--Manuscript Draft--

Manuscript Number:	
Full Title:	Role of apoptosis, autophagy and caspase-3 during post-spawning ovarian remodeling in Oreochromis niloticus
Article Type:	Full-Length Original Research
Keywords:	Apoptosis, Autophagy, Caspase-3, Fish, Heterophagy, Ovary
Corresponding Author:	Nilo Bazzoli, PhD Pontificia Universidade Catolica de Minas Gerais Belo Horizonte, MG BRAZIL
Corresponding Author Secondary Information:	
Corresponding Author's Institution:	Pontificia Universidade Catolica de Minas Gerais
Corresponding Author's Secondary Institution:	
First Author:	Rafael Magno Costa Melo, PhD
First Author Secondary Information:	
Order of Authors:	Rafael Magno Costa Melo, PhD
	Yuri Simões Martins, PhD
	Ronald Kennedy Luz, PhD
	Elizete Rizzo, PhD
	Nilo Bazzoli, PhD
Order of Authors Secondary Information:	
Abstract:	Apoptotic cell death is an essential process to eliminate cells during the development and tissue remodeling of multicellular organisms. Caspase-3 is a key effector molecule of the apoptotic program. Autophagy involves degradation and recycling of cellular components to maintain homeostasis and, under certain conditions, may lead to cell death. The present study investigated the apoptosis and autophagy during ovarian tissue remodeling after spawning in Nile tilapia Oreochromis niloticus. Breeding females were kept in controlled conditions and ovarian samples were collected weekly for morphological, TUNEL assay, immunofluorescence for caspase-3 and morphometric analysis. During the post-spawning follicular growth, a low occurrence of apoptosis in granulosa and theca cells was detected in primary and secondary growth follicles. At 0-3 days post-spawning, post-ovulatory follicles exhibited granulosa cells with intense synthesis activity, various autophagosomes and autolysosomes for cell clearance and high rates of apoptosis. At 7-10 days, post-ovulatory follicles showed granulosa cells with abundant autophagic machinery and lower apoptosis. Early atretic follicles showed granulosa cells containing numerous synthesis organelles, heterophagous activity for phagocytosis of the yolk and low apoptosis. In advanced atresia, granulosa cells exhibited decreased synthesis activity accompanied by increased apoptosis and autophagic organelles. In late atretic follicles, the granulosa cells presented a markedly electron-lucid cytoplasm and higher rates of apoptosis. We concluded that autophagy and apoptosis act cooperatively and play a fundamental role in the post-spawning ovarian recovery in Nile tilapia, especially during follicular regression. Moreover, apoptosis plays an important function in the homeostasis of growing follicles after spawning.

Role of apoptosis, autophagy and caspase-3 during post-spawning ovarian remodeling in *Oreochromis niloticus*

Authors: Rafael M. C. Melo[1], Yuri S. Martins[1], Ronald K. Luz[2], Elizete Rizzo[1], Nilo Bazzoli[3,*]

Affiliations: [1]Departamento de Morfologia, Instituto de Ciências Biológicas, Universidade Federal de Minas Gerais, Belo Horizonte, Minas Gerais, Brazil; [2]Laboratório de Aquacultura, Escola de Veterinária, Universidade Federal de Minas Gerais, Belo Horizonte, Minas Gerais, Brazil; [3]Programa de Pós-graduação em Zoologia de Vertebrados, Pontifícia Universidade Católica de Minas Gerais, Belo Horizonte, Minas Gerais, Brazil.

***Corresponding author**: Nilo Bazzoli, Programa de Pós-graduação em Zoologia de Vertebrados, PUC Minas, Av. Dom José Gaspar, 500, postal address: 30535-610, Belo Horizonte-MG, Brazil. Phone and fax numbers: +55 31 3319-4936; e-mail: bazzoli@pucminas.br

Abstract

Apoptotic cell death is an essential process to eliminate cells during the development and tissue remodeling of multicellular organisms. Caspase-3 is a key effector molecule of the apoptotic program. Autophagy involves degradation and recycling of cellular components to maintain homeostasis and, under certain conditions, may lead to cell death. The present study investigated the apoptosis and autophagy during ovarian tissue remodeling after spawning in Nile tilapia *Oreochromis niloticus*. Breeding females were kept in controlled conditions and ovarian samples were collected weekly for morphological, TUNEL assay, immunofluorescence for caspase-3 and morphometric analysis. During the post-spawning follicular growth, a low occurrence of apoptosis in granulosa and theca cells was detected in primary and secondary growth follicles. At 0-3 days post-spawning, post-ovulatory follicles exhibited granulosa cells with intense synthesis activity, various autophagosomes and autolysosomes for cell clearance and high rates of apoptosis. At 7-10 days, post-ovulatory follicles showed granulosa cells with abundant autophagic machinery and lower apoptosis. Early atretic follicles showed granulosa cells containing numerous synthesis organelles, heterophagous activity for phagocytosis of the yolk and low apoptosis. In advanced atresia, granulosa cells exhibited decreased synthesis activity accompanied by increased apoptosis and autophagic organelles. In late atretic follicles, the granulosa cells presented a markedly electron-lucid cytoplasm and higher rates of apoptosis. We concluded that autophagy and apoptosis act cooperatively and play a fundamental role in the post-spawning ovarian recovery in Nile tilapia, especially during follicular regression. Moreover, apoptosis plays an important function in the homeostasis of growing follicles after spawning.

Keywords Apoptosis, Autophagy, Caspase-3, Fish, Heterophagy, Ovary

Introduction

Programmed cell death is a genetically regulated process that plays a fundamental role during the development and homeostasis of multicellular organisms (Kerr et al. 1972; Jenkins et al. 2013). Evidence from several experimental models shows that multiple programs of cell death can be triggered, depending on the circumstances (Assunção Guimarães and Linden 2004; Degterev and Yuan 2008). The study of different mechanisms of cell death is important for understanding many diseases and biological processes (Nixon 2007; Bolt and Klimecki 2012; Chen et al. 2014).

Apoptosis affects single cells that detached from the surrounding cells and the basement membrane. This type of cell death, highly conserved during evolution, is characterized by fragmentation of internucleosomal DNA and cell fragmentation forming apoptotic bodies, which are engulfed by professional phagocytes or neighboring cells, thus avoiding an inflammatory reaction (Bangs et al. 2000; Drummond et al. 2000). The main effectors of apoptosis are caspases that activate Ca^{2+}/Mg^{2+}-dependent endonucleases, which cleaves the DNA into fragments of 180-200 base pairs (Huettenbrenner et al. 2010). Among the caspases, caspase-3 (Casp3) is a key effector molecule of the apoptotic program being responsible for the proteolytic cleavage of a wide variety of cellular proteins that lead to typical morphological changes of apoptosis (Brentnall et al. 2013).

Autophagy is a complex catabolic program genetically regulated and evolutionarily conserved from yeast to humans. Its main function is to recycle cytoplasmatic organelles and long-life proteins, or malfunctioning proteins, through the lysosomal machinery (Cao and Klionsky 2007; Kang et al. 2011). The relationship between apoptosis and autophagy is complex. In some circumstances, autophagy is a form of adaptation to cellular stress by suppressing apoptosis, while in other conditions it can induce different ways of signaling cell death (Mizushima et al. 2008; Maiuri et al. 2010). Autophagy has specific and context-

dependent functions in cell death and may promote both cell death by caspase-dependent apoptosis and non-apoptotic cell death when caspases are inhibited (Lockshin and Zakeri 2004; Denton et al. 2012).

Post-spawning fish ovaries are excellent experimental models for studying the mechanisms of programmed cell death, especially due to tissue remodeling involving follicular growth and regression for the start of a new reproductive cycle. The growth of ovarian follicles involves two distinct phases: primary and secondary growths. During primary growth, nuclear and cytoplasmic changes occur in the oocytes as well as cortical alveoli accumulation. Secondary growth, influenced by sex hormones, is characterized by the accumulation of yolk globules in the ooplasm leading to a large increase in the follicles' diameter (Lubzens et al. 2010; Melo et al. 2014). After spawning, fish ovaries exhibit post-ovulatory follicles (POF) comprising a basement membrane that separates the granulosa cells from the theca (Santos et al. 2005). In contrast to the corpus luteum of mammals, POF have no hormonal activity in oviparous teleosts and are rapidly reabsorbed during post-spawning ovarian remodeling (Santos et al. 2008a). In fish ovary, the vitellogenic follicles that are not spawned during the reproductive period become atretic follicles and are reabsorbed in a long physiological process (Santos et al. 2008b, Thomé et al. 2009).

Tilapias are the second most important group of fish cultivated in aquaculture worldwide and the Nile tilapia *Oreochromis niloticus* (Linnaeus, 1758) is the main species of tilapia currently farmed (FAO, 2014). The Nile tilapia is an important experimental model for reproductive biology studies due to the spawning in different environmental conditions, adaptability to various culture systems, and resistance to diseases and infections (Little and Hulata 2000). In captivity, females of *O. niloticus* asynchronously spawn every 3 or 4 weeks and the interspawning interval can be influenced by lineage, age and size of fish, temperature,

sex ratio, stocking density, nutritional status, and photoperiod (Coward and Bromage 2000; Lapeyre et al. 2010).

Despite recent studies on the processes of cell death in the functioning of the ovaries in vertebrates (Sundaresan et al. 2007; Choi et al. 2011; Matsuda et al. 2012; Morais et al. 2012), several aspects of the interaction between autophagy and apoptosis during ovarian development and regression have not yet been elucidated. Thus, the aim of this study was to analyze the role of apoptosis, autophagy and caspase-3 during tissue remodeling in the ovaries of *O. niloticus* after spawning.

Materials and methods

Fish stocking and sampling

The experiment was conducted at the Aquaculture Laboratory of the Veterinary School of the Federal University of Minas Gerais (UFMG), southeastern Brazil, during the months of November and December 2010. The research was approved by the Ethics Committee of Animal Experimentation (CETEA) at UFMG. The lineage of *O. niloticus* used in this study originated from the Chitralada Nile tilapia line introduced to Brazil from Thailand in the 1990s. For the reproduction, a breeding stock (age between 12 and 18 months) of adult males [35.37 ± 2.46 cm of total length (TL) and 714.73 ± 107.78 g of body weight (BW)] and females (34.15 ± 2.94 cm TL and 647.57 ± 139.06 g BW), previously kept under captive conditions, were distributed in eight 1 m³ tanks with a water temperature between 26 and 28ºC at a ratio of 2 male to 6 females. After 3 days stocked, the oral cavity of the breeding females was inspected for signs of spawning, and from those which had reproduced, the offspring were taken to prevent mouth-brooding. Then, twelve spawned females were transferred and kept in a 5 m^3 tank with geomembrane liner, heaters with thermostat for maintaining the temperature, continuous supplementary aeration by an air diffuser, and a

photoperiod of 12 h light: 12 h dark (L:D). The fish were fed *ad libitum* twice a day with commercial feed (32 % crude protein), and 30 minutes after feeding the remnants were collected. Females were handled in the absence of males during the experiment, thus avoiding the influence of conspecific factors. The water's physicochemical parameters were monitored weekly (temperature: 29.5 ± 1.5°C, dissolved oxygen: 6.70 ± 1.46 mg l^{-1}, pH: 7.68 ± 0.31, conductivity: 0.28 ± 0. 05 mS cm^{-1}, total dissolved solids: 0.16 ± 0.03 g l^{-1}, salinity: 0.12 ± 0.02 ppt, and turbidity: 1.71 ± 0.38 NTU).

In order to examine post-spawning ovarian remodeling, three females were collected weekly: 0 to 3 days after spawning, 7 to 10 days after spawning, 14 to 17 days after spawning and 21 to 24 days after spawning. Fish were killed by transversal section of the spinal cord following the ethical principles established by the Brazilian College of Animal Experimentation (COBEA). For each female, TL, BW and gonad weight (GW) were obtained, and the gonadosomatic index (GSI) was calculated: 34.89 ± 2.64 cm TL; 661.14 ± 161.83 g BW; 12.96 ± 6.34 g GW; 1.93 ± 0.76 GSI; respectively. Serial samples of the middle region of the ovaries of each specimen were collected for morphological and quantitative analyses employing a variety of techniques.

Light and transmission electron microscopy

For histology, samples of the ovaries (n = 12) were fixed in Bouin's fluid for 24 h at room temperature and then embedded in paraffin. Transverse histological sections of 5 µm thickness were mounted on glass slides and stained with hematoxylin-eosin (HE), Gomori's trichrome (GT), and periodic acid-Schiff (PAS) counterstained with hematoxylin.

For transmission electron microscopy, ovarian samples were fixed in modified Karnovsky's solution (2.5% glutaraldehyde and 2% paraformaldehyde) buffered in 0.1 M phosphate pH 7.3 for 12 h at 4ºC. The samples were post-fixed in 1% osmium tetroxide with

1.5% potassium ferrocyanide for 2 h, and then embedded in Epon/Araldite plastic resin. Ultrathin sections were obtained with a diamond knife and stained with uranyl acetate and lead citrate, and examined using a Tecnai G2-12 Spirit transmission electron microscope at 120 kV (FEI Company, Hillsboro, OR, USA).

In-Situ TUNEL assay

Ovarian samples (n = 12) were fixed in 4% paraformaldehyde solution in 0.1 M phosphate buffer for 24 h at 4ºC, embedded in paraffin, sectioned (5 µm thickness), and submitted to TUNEL (Terminal transferase-mediated dUTP Nick-End Labeling) assay, using the TdT-FragEL DNA fragmentation detection kit QIA 33 (Calbiochem, San Diego, CA, USA) following the manufacturer's protocol. Briefly, the sections were washed in TRIS buffer saline pH 7.6 (TBS), treated with 20 µg/ml proteinase K in 0.01 M Tris-HCl buffer at pH 8 for 20 min, and then treated with 3% hydrogen peroxide (H_2O_2) in TBS for 30 min to inactivate the endogenous peroxidase. The sections were then incubated with terminal deoxynucleotidyl transferase (TdT) and biotinylated deoxynucleotides for 3 h at 37ºC. Sections were incubated with peroxidase-conjugated streptavidin for 45 min at room temperature, developed with diaminobenzidin (DAB, Sigma Aldrich's Corp., St. Louis, MO, USA) in TBS for 8 min, and counterstained with hematoxylin. The negative control excluded treatment with TdT/labeled deoxynucleotides.

Immunofluorescence

Ovarian samples (n = 12) were fixed in 4% paraformaldehyde solution in 0.1 M phosphate buffer for 24 h at 4ºC, embedded in paraffin, sectioned at 5 µm thickness and submitted to immunofluorescence reaction for detection of Casp3 (mouse anti-caspase-3 monoclonal antibody, clone E-8, dilution 1:200, supplier sc-7272, Santa Cruz Biotechnology,

Santa Cruz, CA, USA). The antigen retrieval was performed in citrate buffer (pH 6.0) for 5 min after boiling in a microwave oven. Next, the sections were incubated with 3% H_2O_2 in methanol to inactivate endogenous peroxidase. For permeabilisation and to block unspecific staining, blocking buffer (2% bovine serum albumin + 0.05% Triton X-100 + 0.01% Tween 20) with 10% of normal horse serum was used for 45 min. Next, primary antibody was applied to the sections overnight in a humidified chamber at 4°C. For immunofluorescence, the sections were incubated with a secondary antibody ALEXA 488 (goat anti-rabbit IgG, 1:200, A11034, Life Technologies, Carlsbad, CA, USA). For the negative control, the treatment with the primary antibody was omitted. Fluorescence images were obtained using a 510 META Laser Scanning Confocal Microscope (Zeiss, Oberkochen, Germany) and processed with ImageJ software.

Western blot

In order to determine the molecular weight and specificity of the Casp3 antibody used in immunofluorescence, 300 mg of the ovary (n = 4) were placed in 0.9% NaCl containing protease inhibitors (Sigma Aldrich), and the tissues were homogenized and sonicated. After sonication, the lysates were centrifuged at 14,000 g for 30 min. The supernatants were collected and then frozen at -80°C. The protein samples were diluted to 1:2 in a solution of 10% sodium dodecyl sulfate (SDS, Sigma Aldrich), 2% glycerol and 10% bromophenol blue in 0.5 M Tris buffer (pH 6.8), and after this the samples were boiled for 5 min. Denatured 12% SDS polyacrylamide mini-gels were prepared and 20 µl samples were loaded into the wells. High-molecular-weight markers (Sigma Aldrich) were run parallel to the samples. The separated proteins were transferred onto a nitrocellulose membrane for 75 min, and the strips were blocked with 1% bovine serum albumin (BSA) (Sigma Aldrich) in PBS for 1 h at room temperature. Then the strips were incubated for 120 min at room temperature with the primary

antibody caspase-3 (mouse anti-caspase-3 monoclonal antibody (E-8), 1:200, sc-7272, Santa Cruz Biotechnology). After incubation, the strips were washed three times with TBS 0.05% Tween solution and then incubated for 1 h in biotinylated anti-mouse IgG secondary antibody (Vectastain ABC Kit, PK6102, 1:200) at room temperature. The strips were washed three times with TBS 0.05% Tween solution and incubated in streptavidin solution (Thermo Scientific, TS-125-HR) for 15 min. These strips were then washed three times with TBS 0.05% Tween solution and incubated with DAB (Sigma Aldrich), chloramphenicol (Sigma Aldrich) and hydrogen peroxide (Sigma Aldrich) for 1 minute and washed in water. In order to ensure equal loading of gel and normalize the signals of the protein of interest, the same protocol was used to examine the expression pattern of the loading control antibody PCNA (mouse anti-PCNA monoclonal antibody, clone PC-10, dilution 1:200, supplier sc-56, Santa Cruz Biotechnology). Finally, the strips of protein of interest (Casp3) and loading control (PCNA) were scanned with an Epson Perfection 4990 photo scanner.

Morphometric analyses

The area (F_A) of the early (PG_E) and late (PG_L) primary growth, early (SG_E) and late (SG_L) secondary growth, post-ovulatory (POF) and atretic (AF) follicles was calculated with Motic Images Plus 2.0 software. Moreover, the height (GC_H) of the granulosa cells in SG_L, POF, and AF was also measured. The relative proportion (%) of follicles containing apoptotic cells stained by TUNEL was calculated for each ovarian follicle. The apoptotic index ($I_A = 100\ C_A\ C^{-1}$, where C_A = apoptotic cells labeled by TUNEL and C = whole granulosa cells) was determined for the granulosa cells in POF and AF, according to Santos et al. (2005). The TUNEL relative proportion and the F_A, FC_H and I_A values were calculated using 40 follicles for each development/regression stage.

Statistical analyses

The data were statistically evaluated using Minitab 16.1 and the graphics produced with GraphPad Prism 6.03. Results were considered significant at the 95% confidence interval and the values were expressed as mean ± S.D. The data showed a normal distribution, and hence, a one-way ANOVA followed by Tukey's *post hoc* test was used to compare the mean values of F_A, FC_H and I_A of the follicles. Only the values of the POF follicles were analyzed by Student's t-test. Pearson's coefficient was used to determine the degree of correlation between the morphometric parameters of the POF and AF.

Results

Primary and secondary growth

After spawning, ovaries of *O. niloticus* showed numerous follicles in primary and secondary growth (Fig. 1a) besides germ cells, POF and AF. The PG_E follicle presented a central nucleus with one nucleolus and intensely basophilic cytoplasm, while the PG_L follicle has a nucleus with several nucleoli and less basophilic cytoplasm (Fig. 1a, c, e). Electron microscopy of the envelope layers of follicles in primary growth showed an early formation of the zona radiata and squamous granulosa cells supported by a thick basement membrane adjacent to a developed theca (Fig. 1b).

The SG_E possessed a central nucleus with several nucleoli close to the nuclear envelope and the appearance cortical alveoli in the ooplasm periphery, while the SG_L exhibited ooplasm filled with spherical yolk globules, small cortical alveoli and conspicuous lipid vesicles (Fig. 1a, c, e). Follicles in secondary growth exhibited a zona radiata with two layers, prismatic granulosa cells supported by a basement membrane and theca cells resembling fibroblasts (Fig. 1d). In contrast, dying cells observed in growing follicles showed typical features of cell death by apoptosis, such as compacted chromatin attached to the

nuclear envelope, loss of adhesion to the basement membrane, and formation of membrane blebs on the cell's surface (Fig. 1f).

The area of the follicles PG_E (F = 8. 192, p = 0. 0001), PG_L (F = 6. 468, p = 0. 0006) and SG_L (F = 32. 947, p < 0. 0001) increased significantly during ovarian remodeling, except the area of the SG_E follicle (F = 1.224, p = 0.3021). The GC_H of SG_L follicles showed no significant differences during the period studied (F = 1.727, p = 0.1620) (Table 1).

Autophagy and apoptosis during regression of postovulatory follicles

From 0 to 3 days after spawning, the ovaries of *O. niloticus* showed numerous early post-ovulatory follicles (POF_E), which had a thin layer of theca cells and a single layer of hypertrophied prismatic granulosa cells surrounding a convoluted follicular lumen (Fig. 2a). Electron microscopy of POF_E revealed the start of the detachment of the theca and granulosa cells from basal membrane (Fig. 2b). Cells from the immunological system, such as granulocytes, were recorded close to the follicular layer (Fig. 2b-insert). Granulosa cells showed cytoplasm filled with mitochondria, endoplasmic reticulum and Golgi complex, showing synthesis activity during the initial regression (Fig. 2b, c). The cytoplasm of granulosa cells also showed features of cellular autophagy, including numerous autolysosomes and autophagosomes containing degenerating organelles, as well as vacuoles, electron-dense granules and residual bodies (Fig. 2c, d). Apoptotic cells were frequently observed in the follicular layer, which showed chromatin compacting to the nuclear envelope, loss of cell-cell adhesion, vacuolization and degenerating organelles in the cytoplasm (Fig. 2d).

At 7-10 days post-spawning, the advanced post-ovulatory follicles (POF_A) exhibited a thick theca and granulosa cells in regression (Fig. 2e). The ultrastructure of POF_A revealed intense autophagic activity in the cytoplasm of granulosa cells due to the presence of

numerous autophagosomes, autolysosomes, vacuoles and lysosomes (Fig. 2f, g). In addition, large vacuoles, containing accumulation of autophagosomes, organelle debris, and lamellar structures, were also recorded at this stage of involution of the follicles (Fig. 2g). Apoptotic bodies, containing degenerated organelles, lysosomes, autolysosomes and vacuoles, were observed in follicular layer (Fig. 2h).

Morphometric analyzes showed a significant decrease of F_A ($t = 12.497$, $p < 0.0001$) and GC_H ($t = 22.371$, $p < 0.0001$) during the POF regression (Table 2).

Heterophagy, autophagy and apoptosis during regression of atretic follicles

Follicular atresia in the ovaries of *O. niloticus* was analyzed in 3 stages of regression: early (AF_E), advanced (AF_A), and late (AF_L) atretic follicles. The AF_E presented irregular shape, folding of the zona radiata and early liquefaction of the yolk (Fig. 3a). Electron microscopy of AF_E showed granulosa cells containing numerous organelles of protein synthesis, electron-dense granules and lysosomes (Fig. 3b, c). Some granulosa cells presented nuclei with euchromatin and multilamellar bodies in the cytoplasm (Fig. 3b, d). During early atresia, granulosa cells remained strongly adhered to adjacent cells through adhesion junctions (Fig. 3d-inset).

During advanced atresia, prismatic hypertrophied granulosa cells exhibited intense heterophagous activity, especially engulfing the liquefied yolk and the degenerating zona radiata (Fig. 3e). In AF_A, granulosa cells exhibited membranous structures and degenerating organelles in the cytoplasm and typically apoptotic nuclei (Fig. 3f, g). Granulocytes were commonly observed in the follicular layer during advanced atresia (Fig. 3f-inset). Autophagy was detected in granulosa cells by the presence of large lysosomes and autophagosomes containing degenerating mitochondria and electron-dense granules (Fig. 3g, h).

The AF_L exhibited granulosa and theca cells in regression and complete reabsorption of the yolk and the zona radiata (Fig. 3i). This follicle showed decreased synthesis activity of the granulosa cells and an increase of electron-lucid cells with cytoplasm scarce in organelles. Large multilamellar bodies, membrane structures, multivesicular bodies, few mitochondria and endoplasmic reticulum were observed in the granulosa cells (Fig. 3j). Markedly electron-lucid cells, with euchromatin, rupture of the nuclear envelope, and degenerate organelles in the scarce cytoplasm were frequently registered in late atresia (Fig. 3k). Apoptotic bodies were also detected in the follicular layer (Fig. 3l).

Along follicular atresia, some AF persisted with an apparently intact zona radiata, or with only small slits, even after complete resorption of the yolk and granulosa cells (Fig. 3M-O). Yellow bodies were often recorded in the ovaries of *O. niloticus*, featuring the complete involution of AF (Fig. 3P).

The AF showed a significant decrease of F_A ($F = 135.480$, $p < 0.0001$) and GC_H ($F = 32.234$, $p < 0.0001$) during follicular regression (Table 2).

DNA fragmentation, caspase-3 and apoptotic index

The TUNEL assay from the ovary sections of *O. niloticus* detected DNA fragmentation in some granulosa cells and theca of 2.2% PG_L, 5.9 % SG_E, and 21.4 % SG_L follicles during the period studied (Table 1) (Fig. 4a, b). Casp3 immunoreactivity was frequently observed in the germinal epithelium and in some granulosa cells of follicles in secondary growth (Fig. 4c, d).

All POF and AF analyzed at different stages of involution exhibited apoptotic cells in the granulosa cell layer. In POF_E, the TUNEL reaction mainly labeled the granulosa cells, and apoptotic bodies were frequently observed in the follicular lumen (Fig. 4e). Immunofluorescence for Casp3 strongly labeled the granulosa cells (Fig. 4f, g). In POF_A,

apoptotic cells and apoptotic bodies, revealed by TUNEL, were detected in granulosa cells and in some theca cells (Fig. 4h). At this stage of involution of POF, the immunoreactivity for Casp3 was less intensely detected in the granulosa cells (Fig. 4i, j). During involution of the POF, the I_A of granulosa cells showed a significant decrease ($t = 67.031$, $p < 0.0001$) (Table 2), with a significant positive correlation with F_A ($r = 0.794$, $p < 0.0001$) and the GC_H ($r = 0.919$, $p < 0.0001$).

During initial atresia, the TUNEL assay detected DNA fragmentation in the granulosa cells, whereas theca cells were rarely marked (Fig. 4k). The immunoreactivity for Casp3 also labeled some granulosa cells of AF_E (Fig. 4l, m). In AF_A, the TUNEL reaction mainly labeled granulosa cells, as well as immunostaining for Casp3, which more intensely labeled the granulosa cells of these follicles (Fig. 4n-p). During late atresia, the TUNEL assay and Casp3 immunostaining labeled remaining granulosa cells (Fig. 4q, r). The I_A of granulosa cells exhibited a significant increase during AF involution ($F = 702.411$, $p < 0.0001$) (Table 2), with a significant negative correlation with F_A ($r = -0771$, $p < 0.0001$) and the GC_H ($r = -0579$, $p < 0.0001$). In Western blotting, the band detected by the antibody Casp3 was intense around 20 kDa (Fig. 4s).

Discussion

After spawning in captivity, mature follicles of Nile tilapia may follow two distinct paths. The spawned follicles become POF, which rapidly involute with the aid of autophagic mechanisms and high rates of follicular apoptosis. Non-spawned follicles become AF, which regress more slowly through heterophagic, autophagic mechanisms and lower rates of apoptosis. During ovarian remodeling, apoptosis and autophagy play a key role in regression and removal of POF and AF, as well as in tissue homeostasis for follicular growth.

The *O. niloticus* follicles in primary and secondary growth grew significantly during post-spawning ovarian remodeling. However, we detected a low occurrence of apoptosis in granulosa and theca cells during follicular growth. Studies show that during ovarian development in teleosts, high rates of apoptosis are observed in unfavorable conditions implying a decrease in the number of vitellogenic follicles (Drevnick et al. 2006; Thomé et al. 2012). The captive conditions in this study were appropriate for gonadal development and reproduction of the Nile tilapia (Coward and Bromage 2000; Lapeyre et al. 2010; Little and Hulata 2010), therefore it is suggested that apoptosis recorded during follicular growth has a physiological role to control the number of cells through the elimination of unwanted cells. In the mammalian ovary, apoptosis is also involved in the removal of granulosa cells of follicles in growth during adult life (Rolaki et al. 2005; Matsuda et al. 2012).

During initial regression, POF and AF showed significant involution of the follicular area and the granulosa cells became highly prismatic with well-established cell interactions. Granulosa cell hypertrophy during follicular involution is possibly related to intense synthesis activity observed in POF_E and AF_E. Organelles such as mitochondria, endoplasmic reticulum, and Golgi are involved in the autophagic machinery and in energy supply to the apoptotic process (Lamb et al. 2013; Chiarelli et al. 2014). Throughout the follicular regression, POF and FA showed a significant reduction in the height of granulosa cells concomitant with an increase of cell clearance promoted by autophagy and a decrease of synthesis organelles in the cytoplasm. Furthermore, the granulosa cells exhibit evident loss of cell-cell and basement membrane adhesion. In the rat's mammary gland, the basement membrane provides survival stimulus for epithelial cell culture and loss of adhesion is a sign of cell death (Pullan et al. 1996).

The ultrastructure of *O. niloticus* POF and AF showed that granulocytes were common in the follicular layer, suggesting a relationship between follicular regression and immune

cells, as has been reported for other groups of vertebrates (Gaytán et al. 1998; Lutton and Callard 2006). In fish ovaries, granulocytes were observed engulfing apoptotic bodies during POF and AF regression (Besseau and Faliex 1994; Drummond et al. 2000). The removal of the apoptotic bodies is important to prevent dead cells releasing cytotoxic agents that can alter tissue homeostasis (Nezis et al. 2002). Multilamellar bodies, commonly detected in the granulosa cells of the AF in *O. niloticus*, were also recorded during the follicular atresia in other teleosts (Santos et al. 2005; Thomé et al. 2009).

In this study, apoptotic cell death in POF and AF was mainly detected in the granulosa layer by TUNEL assay, which showed DNA fragmentation, through Casp3 immunofluorescence and also by the main morphological markers of apoptosis: condensation of chromatin in a growth pattern underlying the nuclear envelope, shrinkage and loss of cell adhesion, and cell fragmentation into apoptotic bodies. Pro-apoptotic events were also recorded during the follicular regression in species of teleosts (Thomé et al. 2009; Morais et al. 2012), birds (Murdoch et al. 2005; Sundaresan et al. 2007) and mammals (Rolaki et al. 2005; Luz et al. 2006), indicating that apoptosis plays a key role during post-spawning ovarian remodeling in vertebrates. Through morphometry, we detected a high rate of apoptosis in granulosa cells of POF_E, unlike the AF which showed an increased apoptosis in the final stages of regression. These findings are corroborated by studies involving the neotropical teleosts *Prochilodus argenteus* and *Leporinus taeniatus* which showed a progressive increase in follicular apoptosis in the POF up to 3 days after spawning followed by a subsequent decrease (Santos et al. 2008a), while AF apoptosis increased during the final regression, which usually occurs 4 to 6 months after spawning (Santos et al. 2008b). However, the values of the apoptotic index found in these studies are markedly lower than those detected during regression of *O. niloticus* POF and AF. This fact is possibly related to the greater follicular area and a shorter interval between spawnings of *O. niloticus* in relation

to the above mentioned species, indicating a more efficient ovarian regeneration in the Nile tilapia to allow a new spawning, and a possible relationship between the apoptotic dynamics and different reproductive strategies used by teleosts.

In *O. niloticus* ovaries, Casp3 presented a molecular weight of 20 kDa, as observed in studies with Casp3 in mammals (Skundric et al. 2006; Sdralia et al. 2009). Casp3 immunofluorescence for this species was performed using antibodies from mammals and the Western blotting technique was used to confirm the specificity of the reaction. Casp3 immunofluorescence was detected along follicular growth and regression, but mainly in the granulosa cells of POF_E and $AF_{A,L}$. This suggests that this protein has different functions during post-spawning ovarian remodeling, which present a more effective role in the early steps of POF and in the final stages of AF. Casp3 activity has been identified during follicular regression in teleosts of tropical and temperate regions (Wood and Van Der Kraak, 2003; Santos et al. 2008a; Morais et al. 2012). In mammals, Casp3 is expressed mainly in theca and luteal cells of healthy luteum bodies and in the granulosa of the AF (Hussein, 2005; Luz et al. 2006). Caspase-independent apoptotic pathways have also been found, including those involving mitochondrial apoptosis-inducing factors and non-caspase proteases, such as cathepsins, granzymes, and endonucleases (Zhang et al. 2003; Denton et al. 2012).

In *O. niloticus* ovaries, granulosa cells' heterophagous activity for yolk and zona radiata phagocytosis was detected mainly in early and advanced atresia, concomitant with a significant reduction in follicular area, showing that heterophagy contributes largely to AF involution. Unlike mammals, phagocytosis of the yolk and other follicle structures by granulosa cells during follicular atresia is well documented in non-mammalian vertebrates (Guraya 1986; Santos et al. 2005). However, some AF showed an intact zona radiata, or with small ruptures during follicular regression, in contrast with AF whose zona radiata is completely degraded and reabsorbed in early stages of atresia, as also reported for other

teleosts (Santos et al. 2008b). Future studies with species that present AF with a persistent zona radiata should be conducted to elucidate which mechanisms are involved in the subsequent removal of this structure.

During the Nile tilapia's follicular regression, autophagosomes or autophagic vacuoles with degenerating organelles were abundant in POF and AF granulosa cells, especially in the final stages of involution. The accumulation of autophagic vacuoles in the cytoplasm, filled with organelles and cytoplasmic material, such as mitochondria, endoplasmic reticulum, and ribosomes, is one of the main morphological markers of autophagy (Lockshin and Zakeri 2004; Nixon 2007). In fish, the formation of autophagosomes during follicular atresia was preceded by a cathepsin-D immunoreactivity in cytoplasmic granules, indicating that this protein is involved in triggering autophagy (Morais et al. 2012). Especially during advanced and late atresia in *O. niloticus*, intense clearance promoted by autophagy became the granulosa cells' cytoplasm to be electron-lucid and scarce in organelles, concomitant with increased of the apoptosis rates. In ovaries of insects, both apoptosis and autophagy operate synergistically to achieve rapid and efficient clearance of cells that are no longer needed, resulting in oocyte maturation without disturbances (Velentzas et al. 2007; Mpakou et al. 2011). Therefore, according to the results of the present study, autophagy may be a reduction mechanism of cellular mass prior to caspase activation during follicular regression. In sea-urchin embryos, autophagy may contribute with the energy for apoptotic execution through its catabolic role in stress conditions (Chiarelli et al. 2014). In fish ovaries, the reaction of Casp3 and beclin-1 in granulosa cells associated with the accumulation of autophagosomes is important in triggering apoptotic cell death during atresia (Morais et al. 2012).

In summary, the findings reported in this study indicate that autophagy and apoptosis work cooperatively for an efficient regression of post-ovulatory and atretic follicles and are essential mechanisms in post-spawning tissue remodeling for beginning of a new reproductive

cycle in ovaries of Nile tilapia. Furthermore, apoptosis plays an important role in the homeostasis of growing follicles after spawning.

Acknowledgments

The authors wish to thank the technicians at the Laboratory of Aquaculture (LAQUA) of the UFMG for their assistance in handling of the fishes; the technicians at the Microscopy Center of UFMG for preparation of the biological material for the electron microscope; the Center for Acquisition and Image Processing (CAPI) of UFMG for assistance during immunofluorescence; to Brazilian institutions CAPES (scholarship), CNPq (grants 482756/2012-8, 306792/2011-7), and FAPEMIG (grant CRA-PPM-00394-13) for financial support; and Paulo Henrique de Almeida Campos-Junior, Hélio Batista dos Santos and Ralph Gruppi Thomé for their valuable support during the execution of the study.

References

Assunção Guimarães C, Linden R (2004) Programmed cell deaths. Apoptosis and alternative deathstyles. Eur J Biochem 271:1638–1650

Bangs P, Franc N, White K (2000) Molecular mechanisms of cell death and phagocytosis in *Drosophila*. Cell Death Differ 7:1027–1034

Besseau L, Faliex E (1994) Resorption of unemitted gametes in *Lithognathus mormyrus* (Sparidae, Teleostei): a possible synergic action of somatic and immune cells. Cell Tissue Res 276:123–132

Bolt AM, Klimecki WT (2012) Autophagy in Toxicology: Self-consumption in times of stress and plenty. J Appl Toxicol 32(7):465–479

Brentnall M, Rodriguez-Menocal L, Guevara RL, Cepero E, Boise LH (2013) Caspase-9, caspase-3 and caspase-7 have distinct roles during intrinsic apoptosis. BMC Cell Biol 14:32

Cao Y, Klionsky DJ (2007) Physiological functions of Atg6/Beclin-1: a unique autophagy-related protein. Cell Res 17:839–849

Chen K, Yang Y, Jiang S, Jiang L (2014) Decreased activity of osteocyte autophagy with aging may contribute to the bone loss in senile population. Histochem Cell Biol 142:285–295

Chiarelli R, Agnello M, Bosco L, Roccheri MC (2014) Sea urchin embryos exposed to cadmium as an experimental model for studying the relationship between autophagy and apoptosis. Mar Environ Res 93:47–55

Choi J, Jo M, Lee E, Choi D (2011) Induction of apoptotic cell death via accumulation of autophagosomes in rat granulosa cells. Fertil Steril 95(4):1482-1486

Coward K, Bromage NR (2000) Reproductive physiology of female tilapia broodstock. Rev Fish Biol Fish 10:1–25

Degterev A, Yuan J (2008) Expansion and evolution of cell death programmes. Nat Rev Mol Cell Biol 9:378–390

Denton D, Nicolson S, Kumar S (2012) Cell death by autophagy: facts and apparent artefacts. Cell Death Differ 19:87–95

Drevnick PE, Sandheinrich MB, Oris JT (2006) Increased ovarian follicular apoptosis in fathead minnows (*Pimephales promelas*) exposed to dietary methylmercury. Aquat Toxicol 79:49–54

Drummond CD, Bazzoli N, Rizzo E, Sato Y (2000) Postovulatory follicle: a model for experimental studies of programmed cell death or apoptosis in teleosts. J Exp Zool 287:176–182

Food and Agriculture Organization of the United Nations (FAO) (2014) Cultured Aquatic Species Information Programme: *Oreochromis niloticus* (Linnaeus, 1758). Available at: http://www.fao.org/fishery/culturedspecies/Oreochromis_niloticus/en

Gaytán F, Morales C, Bellido C, Aguilar E, Sánchez-Criado JE (1998) Ovarian follicle macrophages: is follicular atresia in the immature rat a macrophage-mediated event? Biol Reprod 58:52–9

Guraya SS (1986) The cell and molecular biology of fish oogenesis. In: Sauer HW (ed) Monographs of Developmental Biology. Karger Press, New York, pp 169–180

Huettenbrenner S, Maier S, Leisser C, Polgar D, Strasser S, Grusch M, Krupitza G (2003) The evolution of cell death programs as prerequisites of multicellularity. Mutat Res 543:235–249

Hussein MR (2005) Apoptosis in the ovary: molecular mechanisms. Hum Reprod Update 11:162–178

Jenkins VK, Timmons AK, McCall K (2013) Diversity of cell death pathways: insight from the fly ovary. Trends Cell Biol 332:159–170

Kang R, Zeh HJ, Lotze MT, Tang D (2011) The Beclin-1 network regulates autophagy and apoptosis. Cell Death Differ 18:571–580

Kerr JF, Wyllie AH, Currie AR (1972) Apoptosis: basis biological phenomenon with wide ranging implications in tissue kinetics. Br J Cancer 26:239–257

Lamb CA, Yoshimori T, Tooze SA (2013) The autophagosome: origins unknown, biogenesis complex. Mol Cell Biol 14:759–774

Lapeyre BA, Muller-Belecke A, Horstgen-Schwark G (2010) Increased spawning activity of female Nile tilapia (*Oreochromis niloticus*) (L.) after stocking density and photoperiod manipulation. Aquac Res 41:561–567

Little DC, Hulata G (2000) Strategies for tilapia seed production. In: Beveridge MCM, McAndrew BJ (eds) Tilapias: Biology and Exploitation. Kluwer Academic Publishing, Great Britain, pp 267–326

Lockshin RA, Zakeri Z (2004) Apoptosis, autophagy, and more. Int J Biochem Cell Biol 36:2405–2419

Lubzens E, Young G, Bobe J, Cerdà J (2010) Oogenesis in teleosts: How fish eggs are formed. Gen Comp Endocrinol 165:367–389

Lutton B, Callard I (2006) Evolution of reproductive–immune interactions. Int Comp Biol 46:1060–71

Luz MR, Cesário MD, Binelli M, Lopes MD (2006) Canine corpus luteum regression: apoptosis and caspase-3 activity. Theriogenology 66:1448–1453

Maiuri MC, Criollo A, Kroemer G (2010) Crosstalk between apoptosis and autophagy within the Beclin 1 interactome. EMBO J 29:515–516

Matsuda F, Inoue N, Manabe N, Ohkura S (2012) Follicular growth and atresia in mammalian ovaries: regulation by survival and death of granulosa cells. J Reprod Dev 58(1):44–50

Melo RMC, Martins YS, Teixeira EA, Luz RK, Rizzo E, Bazzoli N (2014) Morphological and quantitative evaluation of the ovarian recrudescence in Nile tilapia (*Oreochromis niloticus*) after spawning in captivity. J Morphol 275:348–356

Mizushima N, Levine B, Cuervo AM, Klionsky DJ (2008) Autophagy fights disease through cellular self-digestion. Nature 451:1069–1075

Morais RDVS, Thomé RG, Lemos FS, Bazzoli N, Rizzo E (2012) Autophagy and apoptosis interplay during follicular atresia in fish ovary: a morphological and immunocytochemical study. Cell Tissue Res 347:467–478

Mpakou VE, Velentzas AD, Velentzas PD, Margaritis LH, Stravopodis DJ, Papassideri IS (2011) Programmed cell death of the ovarian nurse cells during oogenesis of the ladybird beetle *Adalia bipunctata* (Coleoptera: Coccinellidae). Dev Growth Differ 53:804–815

Murdoch WJ, Van Kirk EA, Alexander BM (2005) DNA damages in ovarian surface epithelial cells of ovulatory hens. Exp Biol Med (Maywood) 230:429–433

Nezis IP, Stravopodis DJ, Papassideri I, Nicoud-Robert M, Margaritis LH (2002) Dynamics of apoptosis in the ovarian follicle cells during the late stages of *Drosophila* oogenesis. Cell Tissue Res 307:401–409

Nixon RA (2007) Autophagy, amyloidogenesis and Alzheimer disease. J Cell Sci 120(23): 4081-4091

Pullan S, Wilson J, Metcalfe A, Edwards GM, Goberdhan N, Tilly J, Hickman JA, Dive C, Streuli CH (1996) Requirement of basement membrane for the suppression of programmed cell death in mammary epithelium. J Cell Sci 109:631–642

Rolaki A, Drakakis P, Milingos S, Loutradis D, Makrigiannakis A (2005) Novel trends in follicular development, atresia and corpus luteum regression: role for apoptosis. Reprod Biomed Online 11:93–103

Santos HB, Rizzo E, Bazzoli N, Sato Y, Moro L (2005) Ovarian regression and apoptosis in the South American teleost *Leporinus taeniatus* Lütken (Characiformes, Anostomidae) from the São Francisco Basin. J Fish Biol 67:1446–1459

Santos HB, Thomé RG, Arantes FP, Sato Y, Bazzoli N, Rizzo E (2008a) Ovarian follicular atresia is mediated by heterophagy, autophagy, and apoptosis in *Prochilodus argenteus* and *Leporinus taeniatus* (Teleostei: Characiformes). Theriogenology 70:1449–1460

Santos HB, Sato Y, Moro L, Bazzoli N, Rizzo E (2008b) Relationship among follicular apoptosis, integrin β1 and collagen type IV during early ovarian regression in the teleost *Prochilodus argenteus* after induced spawning. Cell Tissue Res 332:159–170

Sdralia ND, Patmanidi AL, Velentzas AD, Margaritis LH, Baltatzis GE, Hatzinikolaou DG, Stavridou A (2009) The mode of lymphoblastoid cell death in response to gas phase cigarette smoke is dose-dependent. Respir Res 10:82

Skundric DS, Cai J, Cruikshank WW, Gveric D (2006) Production of IL-16 correlates with CD4+ Th1 inflammation and phosphorylation of axonal cytoskeleton in multiple sclerosis lesions. J Neuroinflamm 3:13

Sundaresan NR, Saxena VK, Sastry KVH, Anish D, Saxena M, Nagarajan K, Ahmed KA (2007) Nitric oxide: a possible mediator of ovulation and postovulatory follicle regression in chicken. Anim Reprod Sci 101:351–357

Thomé RG, Santos HB, Arantes FP, Domingos FF, Bazzoli N, Rizzo E (2009) Dual roles for autophagy during follicular atresia in fish ovary. Autophagy 5:117–119

Thomé RG, Domingos FFT, Santos HB, Martinelli PM, Sato Y, Rizzo E, Bazzoli N (2012) Apoptosis, cell proliferation and vitellogenesis during the folliculogenesis and follicular growth in teleost fish. Tissue Cell 44:54–62

Velentzas AD, Nezis IP, Stravopodis DJ, Papassideri IS, Margaritis LH (2007) Apoptosis and autophagy function cooperatively for the efficacious execution of programmed nurse cell death during *Drosophila virilis* oogenesis. Autophagy 3:130–132

Wood AW, Van Der Kraak G (2003) Yolk proteolysis in rainbow trout oocytes after serum-free culture: evidence for a novel biochemical mechanism of atresia in oviparous vertebrates. Mol Reprod Dev 65:219–227

Zhang J-H, Zhang Y, Herman B (2003) Caspases, apoptosis and aging. Ageing Res Rev 2:357–366

Figure captions

Fig. 1 Histological sections stained with hematoxylin-eosin (**a, e**) and Gomori trichrome (**c**), and electron microscopy (**b, d, f**) of ovaries during primary and secondary follicular growth at 0-3 (**a**, **b**), 7-10 (**c**), 14-17 (**d**) and 21-24 (**e**, **f**) days after spawning of *O. niloticus*. **a**, **c, e** Spawned ovaries presenting PG_E and PG_L, SG_E and SG_L follicles along the germinal epithelium (GE). **b** PG_E follicle presenting oocyte (O) surrounded by squamous granulosa cells (GC), thick basal membrane (BM) and developing theca (T). **d** SG_L follicle showing two layers in ZR, cuboidal GC, BM and T. **f** Apoptotic cell in theca layer of SG_L follicle presenting nucleus with compacted chromatin underling the nuclear envelope (white arrows), surface blebbing (B) and loss of cell adhesion (asterisk). *Bars* 100 µm (**a**, **c**, **e**), 1 µm (**b**, **d**, **f**)

Fig. 2 Histological sections stained with Gomori trichrome (**a, e**), and electron microscopy (**b-d, f-h**) of ovaries during early (**a-d**) and advanced (**e-h**) regression of the POF after spawning of *O. niloticus*. **a** At 0-3 days post-spawning, POF_E presented hypertrophied granulosa cells (GC), thin theca cells (T) and a broad convoluted follicular lumen (L). **b** POF_E showing hypertrophied GC with numerous mitochondria (M) and endoplasmic reticulum (ER) in the cytoplasm, and T detaching (asterisk) to a rippled basement membrane (BM). Granulocyte (inset) in the follicular layer. **c** GC presenting double-membrane autophagosomes (AF) containing organelles debris (thin white arrows), autolysosomes (AL), lysosomes (L), vacuoles (V), Golgi (G), residual bodies (RB), M and ER in cytoplasm, and intact nucleus (N). **d** GC showing fragmentation of the nuclear envelope (white arrows), electron-dense granules (EG), large V, L, AL and degenerating organelles (thin white arrow). **e** At 7-10 days post-spawning, POF_A exhibited hypertrophied T, GC in regression and smaller L. **f** POF_A with AL, AF with organelles debris (thin white arrow), few M and dilated ER in GC cytoplasm. **g** GC showing N with compacted chromatin coupled to nuclear membrane, and cytoplasm with

L, AL and large V with accumulation of AF and lamellar structures (thin arrow). **h** Apoptotic body, adjacent to granulosa layer, containing AL, V and degenerating organelles (thin white arrows). *Bars* 200 µm (**a**, **e**), 1 µm (**b-d, f-h**)

Fig. 3 Histological sections stained with hematoxylin-eosin (**a**, **e**, **p**), PAS-hematoxylin (**i, m**) and Gomori trichrome (**n, o**), and electron microscopy (**b-d**, **f-h**, **j-l**) of ovaries during early (**a-d**), advanced (**e-h**) and late (**i-l**) regression of the AF after spawning of *O. niloticus*. **a** AF_E with irregular shape, ripples in the zona radiata (ZR) and yolk (Y) at the beginning of liquefaction. **b** AF_E presenting granulosa cells (GC) with euchromatin in the nucleus (N) and cytoplasm filled of electron-dense granules (EG) and lysosomes (L). **c, d** Numerous endoplasmic reticulum (ER), mitochondria (M), Golgi (G), L, multilamellar bodies (MB) and EG in the cytoplasm of GC. Adhesion junctions connect healthy GC (**d**-inset). **e** In AF_A, the ZR breakdown and also liquefies, and along with the Y, were phagocyted by GC; lipid vesicle (LV). **f** AF_A showing GC with disorganized cytoplasm, containing many degenerating organelles (thin white arrow) and membranous structures (white asterisk), as well as granulocytes in the follicular layer (inset). **g, h** GC with chromatin attached to the nuclear envelope (arrow) and electron-lucid cytoplasm with few organelles, including some ER, large L and autophagosomes (AF), containing EG, M debris and other cytoplasmic materials. **i** AF_L presenting residual Y and GC in regression. **j** AF_L showing GC containing large MB, multivesicular bodies (VB), membranous structures (asterisk) and few organelles, such as ER and M. **k** Highly electron-lucid cell with degenerated organelles (thin white arrow) and multiple smaller compartments in cytoplasm, euchromatin in the nucleus (N) and fragmentation of the nuclear envelope (arrows). **l** GC showing electron-lucid cytoplasm with membranous structures (asterisk), MB and an apoptotic body (AB) with degenerate nucleus and other organelles debris (thin white arrow). **m-o** Some AF showing highly convoluted ZR

relatively intact or with small slits (arrows). **p** Yellow bodies (YB) in ovaries. *Bars* 100 µm (**a**, **i**, **m**, **n**), 200 µm (**e**, **o**, **p**), 1 µm (**b-d**, **f-h**, **j-l**), 0.5 µm (**d**-inset)

Fig. 4 TUNEL reaction (left column), immunofluorescence to caspase-3 (Casp3) (middle column) and merge layers to Casp3 (right column and **r**-inset) of ovaries during post-spawning ovarian remodeling of *O. niloticus*. **a**, **b** TUNEL-positive reaction (arrowheads) in granulosa cells (GC) and theca cells (T) of SG_E and SG_L follicles. **c**, **d** Immunofluorescence for Casp3 (white arrowheads) in GC of SG_L follicles and germinal epithelium cells (inset); zona radiata (ZR). **e** TUNEL-positive reaction (arrowheads) in apoptotic cells and apoptotic bodies (white arrows) in GC of POF_E. **f**, **g** Intense immunofluorescence for Casp3 (white arrowheads) in GC of POF_E, with wide lumen (L). **h** TUNEL-positive cells (arrowheads) and apoptotic bodies (white arrows) were observed in GC and T layers of POF_A. **i**, **j** Discrete immunoreaction for caspase-3 (white arrowheads) in GC of POF_A. **k** GC labeled (arrowheads) by TUNEL reaction in AF_E. **l**, **m** Discrete immunofluorescence for Casp3 (white arrowheads) in GC of AF_E; natural immunofluorescence of the liquefied yolk (Y). **n** TUNEL-positive cells (arrowheads) and apoptotic bodies (white arrow) were observed in GC and T of AF_A; basement membrane (MB). **o**, **p** GC of AF_A moderately immunofluorescent for Casp3 (white arrowheads). **Q**) TUNEL reaction (arrowheads) was observed in GC of AF_L. **r** Moderate immunoreaction for Casp3 in the remaining GC of AF_L. **s** Representative Western blotting of the Casp3 expression and respective PCNA loading control. *Bars* 200 µm (**a-r**), 100 µm (**e**, **h**)

Fig. 1

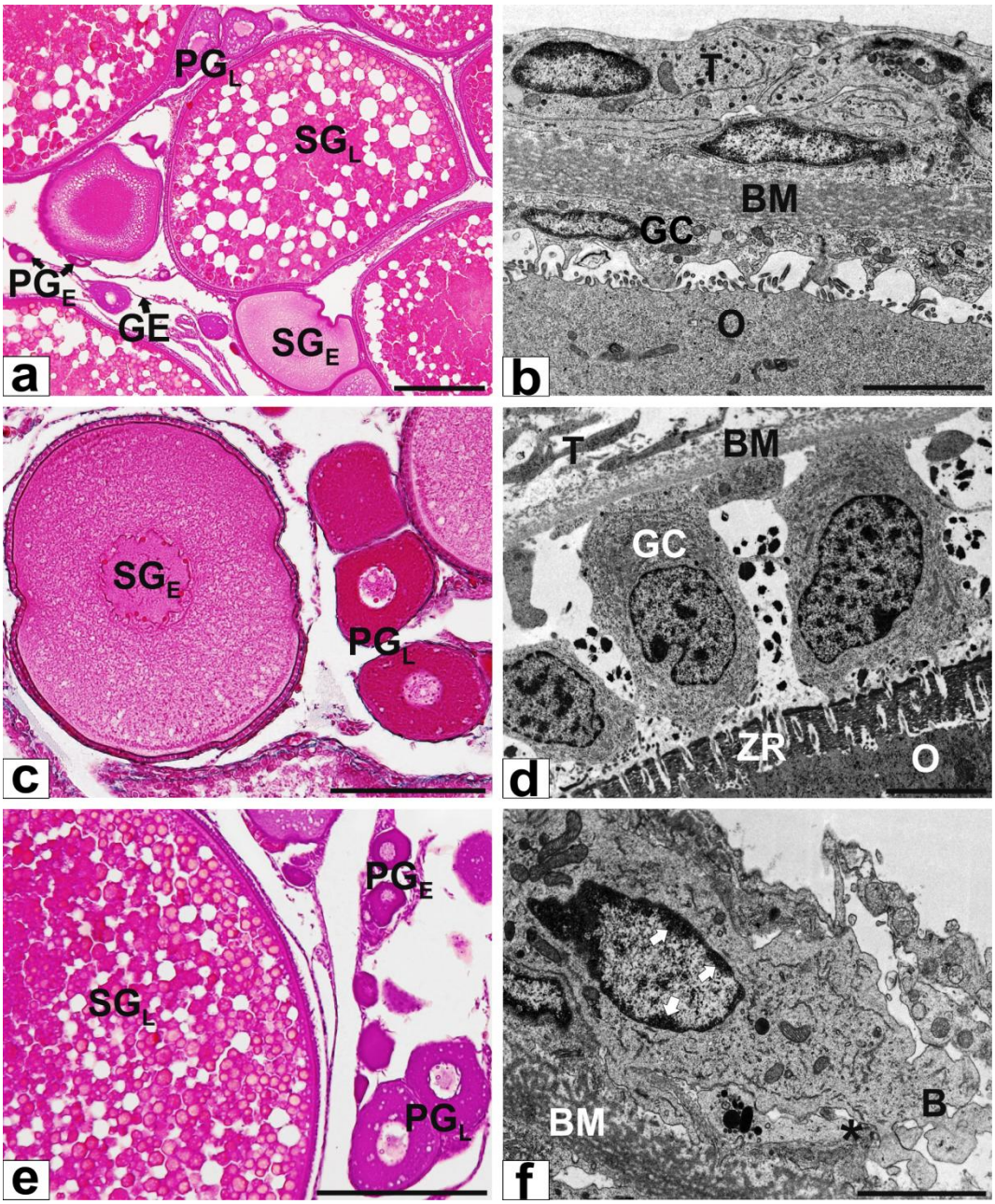
PG_L
SG_L
PG_E
GE
SG_E
a
T
BM
GC
O
b
SG_E
PG_L
c
T
BM
GC
ZR
O
d
PG_E
SG_L
PG_L
e
BM
B
*
f

Fig. 2

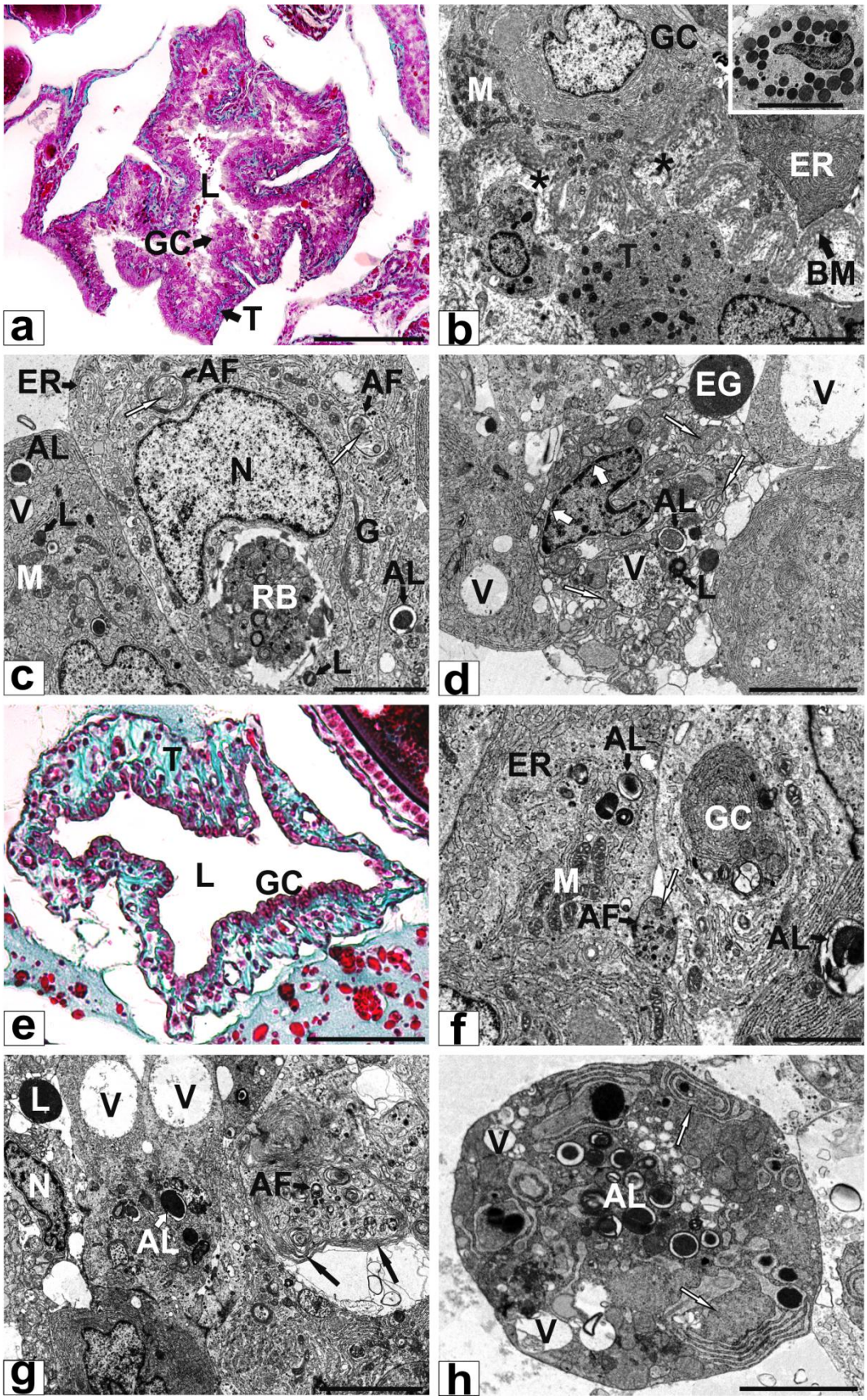
a
L
GC
T
b
GC
M
ER
T
BM
c
ER
AF
AF
AL
N
V
L
G
M
RB
AL
L
d
EG
V
AL
V
V
L
e
T
L
GC
f
ER
AL
GC
M
AF
AL
g
L
V
V
N
AF
AL
h
V
AL
V

Fig. 3

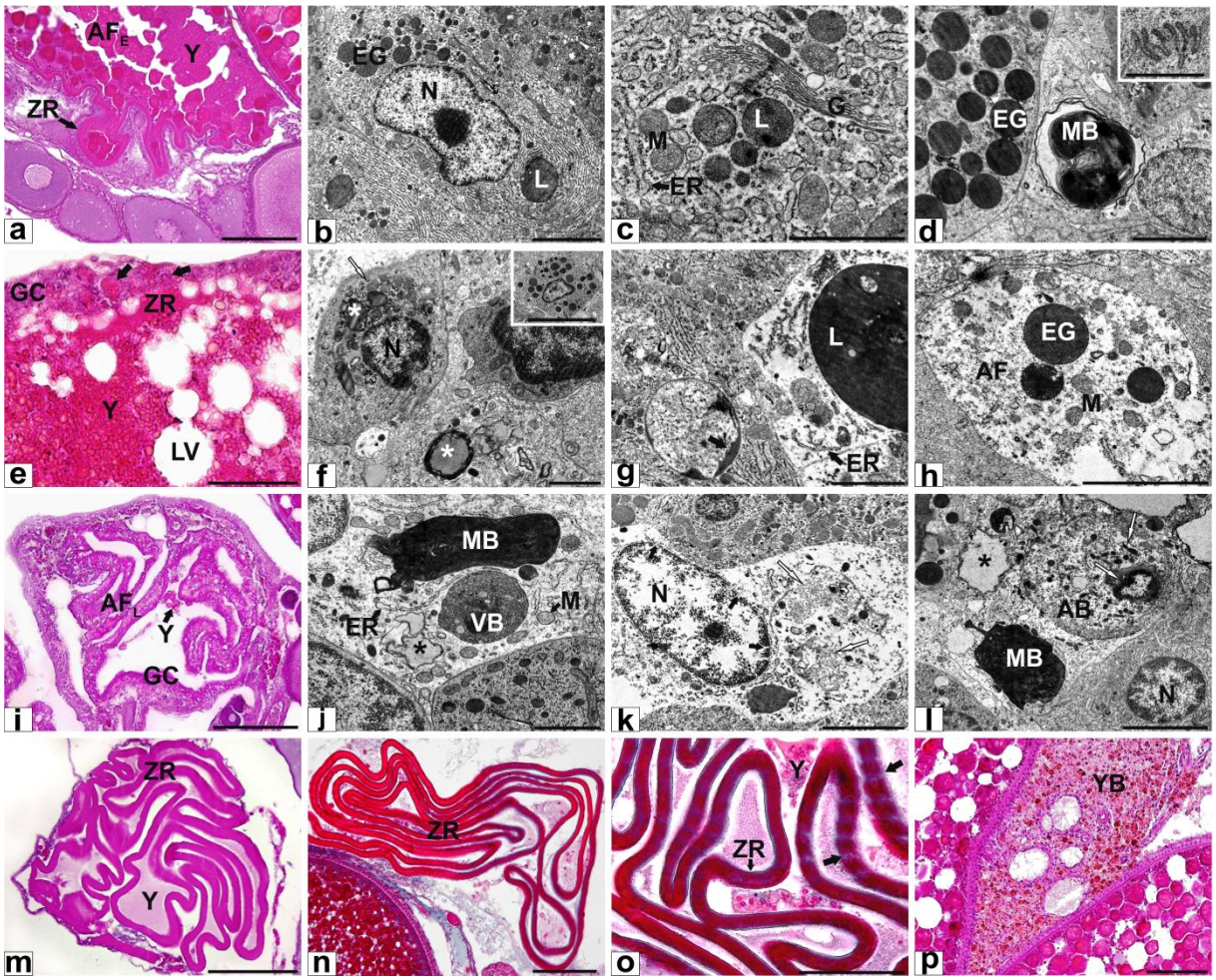
a
AF$_E$
Y
ZR
b
EG
N
L
c
L
G
M
ER
d
EG
MB
e
GC
ZR
Y
LV
f
N
*
*
g
L
ER
h
EG
AF
M
i
AF$_L$
Y
GC
j
MB
VB
M
ER
*
k
N
l
*
AB
MB
N
m
ZR
Y
n
ZR
o
Y
ZR
p
YB

Fig. 4

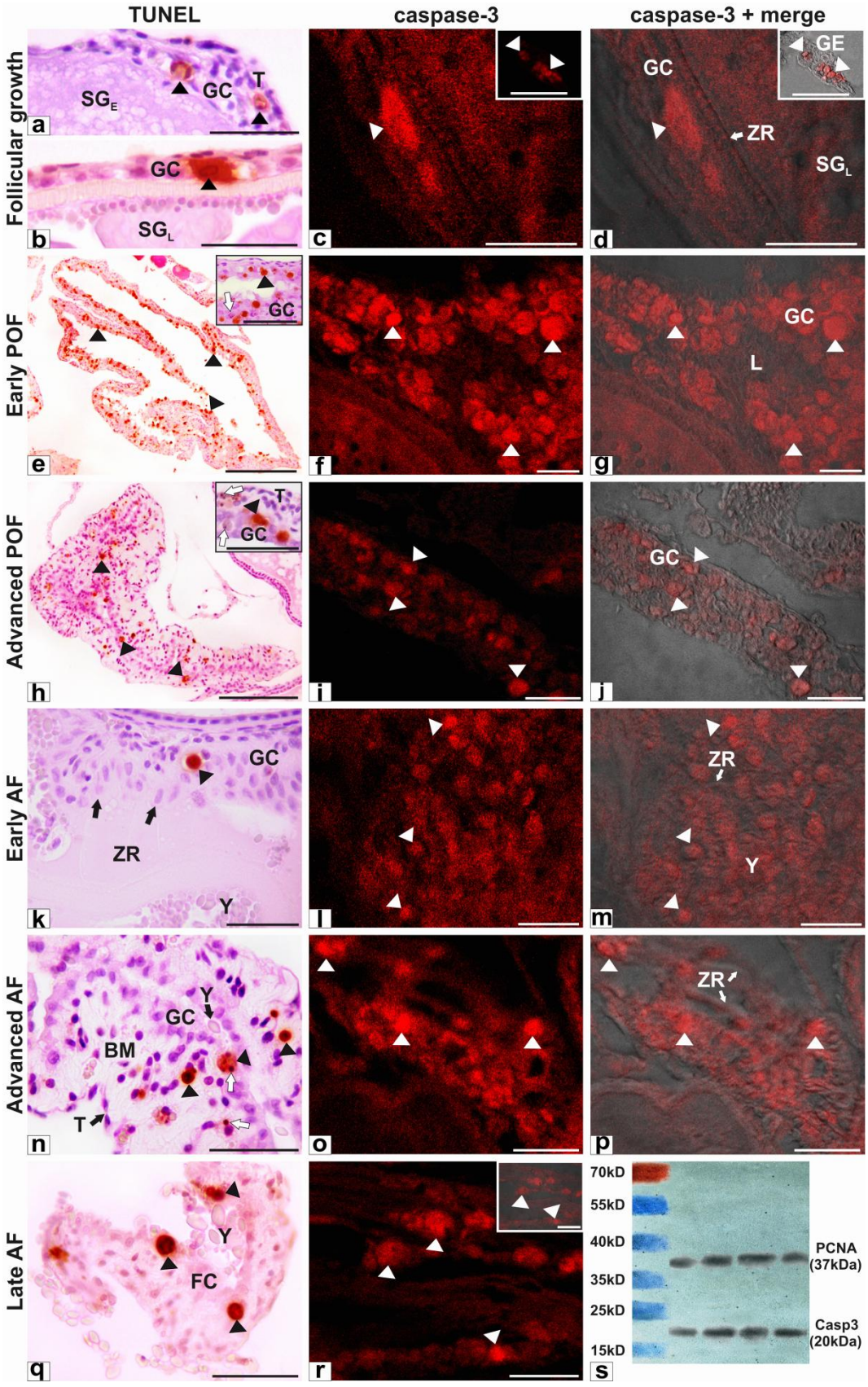
TUNEL
caspase-3
caspase-3 + merge
Follicular growth
Early POF
Advanced POF
Early AF
Advanced AF
Late AF
SG_E
GC
T
SG_L
GE
ZR
L
Y
BM
FC
70kD
55kD
40kD
35kD
25kD
15kD
PCNA (37kDa)
Casp3 (20kDa)
a
b
c
d
e
f
g
h
i
j
k
l
m
n
o
p
q
r
s

Table 1
Click here to download Table: Table 1.docx

Table 1 Follicular area (F_A 10^3 µm²) and TUNEL-positive relative proportion (%) of early (PG_E) and late (PG_L) primary, early (SG_E) and late (SG_L) secondary growth follicles and the height of the granulosa cells (GC_H µm) of SG_L follicle during post-spawning ovarian remodeling in *O. niloticus*

Days	Primary growth			Secondary growth				
	PG_E	PG_L	%	SG_E	%	SG_L	%	GC_H
0-3	1.58 ± 0.58^{b}	8.43 ± 2.58^{b}	-	81.25 ± 47.96^{a}	-	400.95 ± 106.55^{c}	14.6	3.73 ± 0.68^{a}
7-10	2.14 ± 0.75^{a}	11.23 ± 4.60^{a}	2.6	87.42 ± 42.87^{a}	5.3	918.97 ± 239.36^{b}	21.0	3.85 ± 0.66^{a}
14-17	2.17 ± 0.96^{a}	10.21 ± 3.32^{ab}	2.7	84.13 ± 33.65^{a}	6.7	1068.78 ± 772.50^{b}	22.8	3.95 ± 0.75^{a}
21-24	2.54 ± 1.12^{a}	11.74 ± 3.73^{a}	3.5	98.58 ± 47.52^{a}	11.8	1369.15 ± 361.44^{a}	27.2	4.08 ± 0.76^{a}

Values represent means ± S.D. In same column, different letters indicate significant differences ($p < 0.05$)

Table 2
Click here to download Table: Table 2.docx

Table 2 Regression of post-ovulatory (POF) and atretic (AF) follicles during post-spawning ovarian remodeling in *O. niloticus:* follicular area (F_A 10^3 µm²), height of the granulosa cells (GC_H µm) and apoptotic index of the follicular cells (I_A %)

Regression	**F_A**	**GC_H**	**I_A**
Early POF (0-3 days)	108.83 ± 39.63[a]	8.55 ± 1.06[a]	39.08 ± 1.54[a]
Advanced POF (7-10 days)	30.29 ± 3.09[b]	3.93 ± 0.76[b]	14.71 ± 1.71[b]
Early AF	628.34 ± 211.43[a]	8.15 ± 1.90[a]	4.91 ± 1.03[c]
Advanced AF	310.69 ± 56.88[b]	7.35 ± 1.78[a]	9.89 ± 1.08[b]
Late AF	155.09 ± 59.94[c]	5.25 ± 1.26[b]	15.83 ± 1.70[a]

Values represent means ± S.D. During regression of POF or AF, different letters in same column indicate significant differences ($p < 0.05$)

5. DISCUSSÃO

Estudos sobre a dinâmica de regeneração dos ovários após desova em peixes, especialmente em espécies de importância comercial como *O. niloticus*, são essenciais por fornecer subsídios para aquicultura. Esta abordagem também permite conhecer melhor os mecanismos celulares envolvidos na remodelação tecidual ovariana para início de um novo ciclo reprodutivo. Em condições ambientais e/ou de cultivo adequadas para reprodução, a tilápia-do-nilo apresenta desenvolvimento ovariano assincrônico com um curto intervalo (> 1 mês) entre desovas, fecundidade baixa, ovos com grande diâmetro e cuidado parental (Little & Hulata, 2000; Coward & Bromage, 2000), configurando uma estratégia reprodutiva peculiar que lhe permite desovar quase continuamente em diferentes ambientes. Estas características tornam a tilápia-do-nilo um importante modelo experimental para estudos morfofisiológicos da reprodução, além de tornar o seu cultivo mais eficiente e rentável, apesar da baixa fecundidade. Entretanto, esta estratégia reprodutiva também lhe confere um alto potencial invasor nas bacias hidrográficas onde é introduzida, especialmente em ambientes lênticos como reservatórios e lagos naturais, o que pode acarretar alguns impactos negativos sobre fauna de peixes nativos e o ecossistema local (Arthur et al., 2010; Martin et al., 2010).

Logo após a desova, ovários de *O. niloticus* apresentaram folículos ovarianos em todos os estádios de desenvolvimento e predominância de folículos em crescimento primário, enquanto mais de 20% dos folículos já se encontravam na vitelogênese. Após 21 dias de recuperação ovariana, todos os folículos em crescimento aumentaram significativamente de tamanho e os folículos de crescimento completo já predominavam nos ovários, representando 35% dos folículos. As fêmeas de *O. niloticus* também mantiveram um estoque estável de ovogônias e folículos primários durante a remodelação ovariana. Estas características reprodutivas mostraram um rápido crescimento folicular após desova da tilápia-do-nilo, e que

estoques de folículos em crescimento estão constantemente disponíveis para o recrutamento, permitindo, assim, uma rápida recuperação ovariana para a próxima desova. Entretanto, existem tilápias com regeneração ovariana mais eficiente, como *Tilapia zillii*, cujos folículos vitelogênicos ocuparam cerca de 70% dos ovários 8 dias após desova, e o menor intervalo entre desovas foi registrado em apenas 7 dias (Coward and Bromage, 1999). Estas diferenças temporais na remodelação ovariana entre espécies de Tilapiine podem estar relacionadas às diferentes estratégias reprodutivas adotadas pelas espécies, visto que *T. zillii* geralmente desova e cuida da prole no substrato, possui alta fecundidade, ovos menores e ciclo reprodutivo mais curto que espécies que incubam a prole na boca, como a tilápia-do-nilo (Coward and Bromage, 2000).

Ao longo do crescimento folicular em ovários de *O. niloticus*, as células foliculares foram pavimentosas no crescimento primário e cúbicas no crescimento secundário. Isto se deve ao aumento da atividade de síntese das células foliculares e constante interação com o ovócito durante o desenvolvimento dos folículos, além de participação no desenvolvimento da zona radiata. Estudos mostram que, durante o desenvolvimento ovariano de teleósteos, altas taxas de apoptose são observadas em condições desfavoráveis para reprodução (Janz and Van Der Kraak, 1997; Drevnick et al., 2006; Thomé et al., 2012). No presente estudo, uma baixa ocorrência de apoptose nas células foliculares e tecais foi detectada durante o crescimento folicular, indicando que as condições de cultivo utilizadas foram apropriadas ao desenvolvimento gonadal e reprodução da tilápia-do-nilo. Deste modo, sugere-se que a apoptose registrada durante o crescimento folicular tenha um papel fisiológico para controlar o número de células, eliminando células não desejáveis, assim como também observado no teleósteo *Prochilodus argenteus* (Thomé et al., 2010).

Durante a remodelação ovariana pós-desova da tilápia-do-nilo os FPO e FA exibiram significativa regressão da área folicular. Assim como relatado em outros vertebrados não

mamíferos (Guraya, 1986; Santos et al., 2008a), a atividade heterofágica das células foliculares para fagocitose do vitelo e da zona radiata contribuiu para redução da área folicular durante a atresia de *O. niloticus*. A hipertrofia das células foliculares observada nos FPO e FA está possivelmente relacionada com a intensa atividade de síntese durante as etapas iniciais da regressão destes folículos. É importante ressaltar que organelas, como mitocôndrias, retículo endoplasmático e Golgi, estão envolvidas na maquinaria autofágica e no aporte energético para o processo apoptótico (Lamb et al., 2013; Chiarelli et al., 2014). A altura das células foliculares dos FPO e FA reduziu gradativamente ao longo da regressão folicular, acompanhada pela diminuição das organelas de síntese e por um aumento da atividade autofágica no citoplasma.

Autofagossomas ou vacúolos autofágicos com organelas em degeneração foram abundantes nas células foliculares dos FPO e FA durante a remodelação ovariana da tilápia-do-nilo. Especialmente durante a atresia avançada e final de *O. niloticus*, a intensa depuração celular promovida pela autofagia tornou o citoplasma das células foliculares eléctron-lúcido e escasso em organelas, concomitante ao aumento das taxas de apoptose. Em ovários de insetos, apoptose e autofagia atuam sinergicamente para alcançar uma depuração rápida e eficiente de células que não são mais necessárias, resultando em uma maturação ovocitária sem distúrbios (Velentzas et al., 2007; Mpakou et al., 2011). Em embriões de ouriço-do-mar, a autofagia pode contribuir com energia para execução apoptótica através do seu papel catabólico em condições de stress (Chiarelli et al., 2014). Portanto, de acordo com os resultados do presente estudo, autofagia pode ser um mecanismo de redução de massa celular anterior à ativação das caspases durante a involução folicular em ovários de tilápia-do-nilo.

A morte celular apoptótica nos FPO e FA foi detectada principalmente nas células foliculares e, posteriormente, na teca pela reação de TUNEL que mostrou fragmentação do DNA, pela imunohistoquímica para caspase 3 e também pelos principais marcadores

morfológicos de apoptose. Eventos pró-apoptóticos também foram observados durante a involução folicular em diversas espécies de teleósteos (Drummond et al., 2000; Santos et al., 2005; Thomé et al., 2009; Morais et al., 2012), indicando que a apoptose folicular possui um papel fundamental na remodelação ovariana pós-desova em peixes, assim como em outros vertebrados, como aves (Murdoch et al., 2005; Sundaresan et al., 2007) e mamíferos (Rolaki et al., 2005; Luz et al., 2006). Uma alta taxa de apoptose foi observada nas células foliculares dos FPO iniciais, ao contrário dos FA que apresentaram aumento de apoptose folicular nas etapas finais da regressão. Estes resultados são corroborados por estudos envolvendo os teleósteos *P. argenteus* e *Leporinus taeniatus*, que mostraram um aumento progressivo da apoptose folicular nos FPO até 3 dias pós-desova e um posterior decréscimo (Santos et al., 2008b), enquanto nos FA a apoptose aumentou durante a regressão final, que geralmente ocorre de 4 a 6 meses após desova (Santos et al., 2008a). Entretanto, os valores do índice apoptótico encontrados nestes estudos são inferiores aos detectados durante a regressão dos FPO e FA de *O. niloticus*. Este fato está possivelmente relacionado à maior área folicular e menor intervalo entre desovas de *O. niloticus* em relação a estas espécies (Santos et al., 2008a,b), indicando uma participação mais intensa da apoptose na involução folicular da tilápia-do-nilo e uma possível relação entre a dinâmica apoptótica e as diferentes estratégias reprodutivas utilizadas pelos teleósteos.

6- CONCLUSÕES

1. Na tilápia-do-nilo ocorre um rápido crescimento folicular e rápida recuperação ovariana após desova em 21 dias a 29,5 °C;

2. A maior intensidade dos mecanismos e interações celulares nos ovários da tilápia-do-nilo após desova está associada com a sua estratégia reprodutiva, que promove uma rápida e eficiente recuperação ovariana;

3. Apoptose exerce um importante papel no controle das células foliculares e tecais dos folículos ovarianos em crescimento após a desova;

4. Autofagia e apoptose atuam cooperativamente para regressão e eliminação dos folículos pós-ovulatórios e atrésicos nos ovários, exercendo um papel fundamental na remodelação tecidual após desova em ovários de tilápia-do-nilo.

7- REFERÊNCIAS BIBLIOGRÁFICAS

ANDRADE, R.F.; BAZZOLI, N.; RIZZO, E.; SATO, Y. (2001) Continuous gametogenesis in the neotropical freshwater teleost, *Bryconops affinis* (Pisces: Characidae). *Tissue Cell* 33:524–532.

ARTHUR, R.I.; LORENZEN, K.; HOMEKINGKEO, P.; SIDAVONG, K.; SENGVILAIKHAM, B.; GARAWAY, C.J. (2010) Assessing impacts of introduced aquaculture species on native fish communities: Nile tilapia and major carps in SE Asian freshwaters. *Aquaculture* 299:81–88.

ASSUNÇÃO GUIMARÃES, C. & LINDEN, R. (2004) Programmed cell deaths. Apoptosis and alternative deathstyles. *Eur J Biochem* 271:1638–1650.

BANGS, P.; FRANC. N.; WHITE, K. (2000) Molecular mechanisms of cell death and phagocytosis in *Drosophila*. *Cell Death Differ* 7:1027–1034.

BOLT, A.M. & KLIMECKI, W.T. (2012) Autophagy in Toxicology: Self-consumption in times of stress and plenty. *J Appl Toxicol* 32:465–479.

CAMPOS-MENDOZA, A; McANDREW, B.J.; COWARD, K.; BROMAGE, N.R. (2004) Reproductive response of Nile tilapia (*Oreochromis niloticus*) to photoperiod manipulation; effects on spawning periodicity, fecundity and egg size. *Aquaculture* 231:299–313.

CAO, Y. & KLIONSKY, D.J. (2007) Physiological functions of Atg6/Beclin-1: a unique autophagy-related protein. *Cell Res* 17:839–849.

CHIARELLI, R.; AGNELLO, M.; BOSCO, L.; ROCCHERI, M.C. (2014) Sea urchin embryos exposed to cadmium as an experimental model for studying the relationship between autophagy and apoptosis. *Mar Environ Res* 93:47–55.

CHOI, J.; JO, M.; LEE, E.; CHOI, D. (2011) Induction of apoptotic cell death via accumulation of autophagosomes in rat granulosa cells. *Fertil Steril* 95:1482–1486.

COWARD, K. & BROMAGE, N.R. (1998) Histological classification of oocyte growth and the dynamics of ovarian recrudescence in *Tilapia zillii*. *J Fish Biol* 53:285–302.

COWARD, K. & BROMAGE, N.R. (1999) Spawning periodicity, fecundity and egg size in laboratory-held stocks of a substrate-spawning tilapiine, *Tilapia zillii* (Gervais). *Aquaculture* 171:251–267.

COWARD, K. & BROMAGE, N.R. (2000) Reproductive physiology of female tilapia broodstock. *Rev Fish Biol Fish* 10:1–25.

DEBNATH, J.; BAEHRECKE, E.H.; KROEMER, G. (2005) Does autophagy contribute to cell death? *Autophagy* 1:66–74.

DEGTEREV, A. & YUAN, J. (2008) Expansion and evolution of cell death programmes. *Nat Rev Mol Cell Biol* 9:378–390.

DENTON, D.; NICOLSON, S.; KUMAR, S. (2012) Cell death by autophagy: facts and apparent artefacts. *Cell Death Differ* 19:87–95.

DJAVAHERI-MERGNY, M.; MAIURI, M.C.; KROEMER, G. (2010) Cross talk between apoptosis and autophagy by caspase-mediated cleavage of Beclin-1. *Oncogene* 29:1717–1719.

DREVNICK, P.E.; SANDHEINRICH, M.B.; ORIS, J.T. (2006) Increased ovarian follicular apoptosis in fathead minnows (*Pimephales promelas*) exposed to dietary methylmercury. *Aquat Toxicol* 79:49–54.

DRUMMOND, C.D.; BAZZOLI, N.; RIZZO, E.; SATO, Y. (2000) Postovulatory follicle: a model for experimental studies of programmed cell death or apoptosis in teleosts. *J Exp Zool* 287:176–82.

FAO (Food and Agriculture Organization of the United Nations). (2014) Cultured Aquatic Species Information Programme: *Oreochromis niloticus* (Linnaeus, 1758). http://www.fao.org/fishery/culturedspecies/Oreochromis_niloticus/en. Acesso em 11/04/2014.

GRIER, H.J.; URIBE, A.M.C.; PATIÑO, R. (2009) The ovary, folliculogenesis, and oogenesis in teleosts. In: Jamieson BGM (ed). *Reproductive Biology and Phylogeny of Fishes (Agnathans and Neotelestomi)*, Vol. 8A. Enfield, New Hampshire: Science Publishers, pp. 25–84.

GRIER, H.J. (2012) Development of the follicle complex and oocyte staging in red drum, *Sciaenops ocellatus* Linnaeus, 1776 (Perciformes, Sciaenidae). *J Morphol* 273:801–829.

GUNASEKERA, R.M.; SHIM, K.F.; LAM, T.J. (1996) Effect of dietary protein level on spawning performance and amino acid composition of eggs of Nile tilapia, *Oreochromis niloticus*. *Aquaculture* 146:121-134.

GURAYA, S.S. (1986) The cell and molecular biology of fish oogenesis. In: Sauer HW (ed). Monographs of Developmental Biology, vol. 18. New York: Karger Press, pp. 169–180.

HUETTENBRENNER, S.; MAIER, S.; LEISSER, C.; POLGAR, D.; STRASSER, S.; GRUSCH, M.; KRUPITZA, G. (2003) The evolution of cell death programs as prerequisites of multicellularity. *Mutat Res* 543:235–249.

HUSSEIN, M.R. (2005) Apoptosis in the ovary: molecular mechanisms. *Hum Reprod Update* 11:162–178.

JALABERT, B. & ZOHAR, Y. (1982) Reproductive physiology in cichlid fishes, with particular reference to *Tilapia* and *Soratherodon*. In: Pullin RSV, Lowe-McConnell RH (eds). *The Biology and Culture of Tilapias*. Manila: International Center for Living Aquatic Resources Management, pp. 129–140.

JANZ, D.M. & VAN DER KRAAK, G. (1997) Supression of apoptosis by gonadotropin, 17β-estradiol, and epidermal growth factor in rainbow trout preovulatory ovarian follicles. *Gen Comp Endo* 105:186–193.

JENKINS, V.K.; TIMMONS, A.K.; MCCALL, K. (2013) Diversity of cell death pathways: insight from the fly ovary. *Trends Cell Biol* 332:159–170.

KANG, R.; ZEH, H.J.; LOTZE, M.T.; TANG, D. (2011) The Beclin-1 network regulates autophagy and apoptosis. *Cell Death Differ* 18:571–580.

KERR, J.F.R.; WYLLIE, A.H.; CURRIE, A.R. (1972) Apoptosis. A basic biological phenomenon with wide-ranging implications in tissue kinectics. *Br J Cancer* 26:239–257.

KLIONSKY, D.J. (2007) Autophagy: from phenomenology to molecular understanding in less than a decade. *Nat Rev Mol Cell Biol* 8:931–937.

LAMB, C.A.; YOSHIMORI, T.; TOOZE, S.A. (2013) The autophagosome: origins unknown, biogenesis complex. *Mol Cell Biol* 14:759–774.

LEONARDO, A.F.G.; ROMAGOSA, E.; BATLOUNI S.R.; BORELLA, M.I. (2006) Occurrence and significance of ovarian and follicular regression in cachara *Pseudoplatystoma fasciatum* (Linnaeus, 1766): a histology approach. *Arq Bras Med Vet Zootec* 58(5):831–840.

LEONHARDT, J.H. (1997) Efeito da reversão sexual em tilápia-do-nilo, *Oreochromis niloticus* (Linnaeus, 1757). *Tese de Doutorado em Aquicultura*. Universidade Estadual Paulista, Faculdade de Ciências Agrárias e Veterinárias, Jaboticabal, 141p.

LITTLE, D.C. & HULATA G. (2000) Strategies for tilapia seed production. In: Beveridge MCM, McAndrew BJ (eds). *Tilapias: Biology and Exploitation*. Great Britain: Kluwer Academic Publishing, pp. 267–326.

LOCKSHIN, R.A. & ZAKERI, Z. (2004) Apoptosis, autophagy, and more. *Int J Biochem Cell Biol* 36:2405–2419.

LUBZENS, E.; YOUNG, G.; BOBE, J.; CERDÀ, J. (2010) Oogenesis in teleosts: how fish eggs are formed. *Gen Comp Endo* 165:367–389.

LUND, V.X. & FIGUEIRA, M.L.O.A. (1989) *Criação de tilápias*. São Paulo: Livraria Nobel, 63p.

LUZ, M.R.; CESÁRIO, M.D.; BINELLI, M.; LOPES, M.D. (2006) Canine corpus luteum regression: apoptosis and caspase-3 activity. *Theriogenology* 66:1448–1453.

MAIURI, M.C.; CRIOLLO, A.; KROEMER, G. (2010) Crosstalk between apoptosis and autophagy within the Beclin 1 interactome. *EMBO J* 29:515–516.

MARTIN, C.W.; VALENTINE, M.M., VALENTINE, J.F. (2010) Competitive Interactions between Invasive Nile Tilapia and Native Fish: The Potential for Altered Trophic Exchange and Modification of Food Webs. *PlosOne* 5(12):1–6.

MATSUDA, F.; INOUE, N.; MANABE, N.; OHKURA, S. (2012) Follicular growth and atresia in mammalian ovaries: regulation by survival and death of granulosa cells. *J Reprod Dev* 58:44–50.

MELO, R.M.C.; MARTINS, Y.S.; TEIXEIRA, E.A.; LUZ, R.K.; RIZZO, E.; BAZZOLI, N. (2014) Morphological and quantitative evaluation of the ovarian recrudescence in Nile tilapia (*Oreochromis niloticus*) after spawning in captivity. *J Morphol* 275:348–356.

MIZUSHIMA N, LEVINE B, CUERVO AM, KLIONSKY DJ. (2008) Autophagy fights disease through cellular self-digestion. *Nature* 451:1069–1075.

MORAIS, R.D.V.S.; THOMÉ, R.G.; LEMOS, F.S.; BAZZOLI, N.; RIZZO, E. (2012) Autophagy and apoptosis interplay during follicular atresia in fish ovary: a morphological and immunocytochemical study. *Cell Tissue Res* 347:467–478.

MPAKOU, V.E.; VELENTZAS, A.D.; VELENTZAS, P.D.; MARGARITIS, L.H.; STRAVOPODIS, D.J.; PAPASSIDERI, I.S. (2011) Programmed cell death of the ovarian nurse cells during oogenesis of the ladybird beetle *Adalia bipunctata* (Coleoptera: Coccinellidae). *Dev Growth Differ* 53:804–815.

MURDOCH, W.J.; VAN KIRK, E.A.; ALEXANDER, B.M. (2005) DNA damages in ovarian surface epithelial cells of ovulatory hens. *Exp Biol Med* (Maywood) 230:429–433.

NAGL, S.; TICHY, H.; MAYER, W.E.; SAMONTE, I.E.; MCANDREW, B.J.; KLEIN, J. (2001) Classification and Phylogenetic Relationships of African Tilapiine Fishes Inferred from Mitochondrial DNA Sequences. *Mol Phyl Evol* 20(3):361–374.

NIXON, R.A. (2007) Autophagy, amyloidogenesis and Alzheimer disease. *J Cell Sci* 120(23): 4081-4091.

PATIÑO, R. & SULLIVAN, C.V. (2002). Ovarian follicle growth, maturation, and ovulation in teleost fish. *Fish Physiol Biochem* 26:57–70.

POPMA, T.J. & LOVSHIN, L. (1996) *Worldwide Prospects for Commercial Production Of Tilapia*. International Center for Aquaculture and Aquatic Environments. Auburn: Auburn University, Alabama. Research And Development. Series n. 41, 23 p.

QUAGIO-GRASSIOTTO, I.; GRIER, H.G.; MAZZONI, T.S.; NÓBREGA, R.H.; ARRUDA, A.J.P. (2011) Activity of the ovarian germinal epithelium in the freshwater catfish, *Pimelodus maculatus* (Teleostei: Ostariophysi: Siluriformes): Germline cysts, follicle formation and oocyte development. *J Morphol* 272:1290–1306.

RIDHA, M.T. & CRUZ, E.M. (1999) Effect of different broodstock densities on the reproductive performance of Nile tilapia, *Oreochromis niloticus* (L.), in a recycling system. *Aquac Res* 30:203–210.

ROLAKI, A.; DRAKAKIS, P.; MILINGOS, S.; LOUTRADIS, D.; MAKRIGIANNAKIS, A. (2005) Novel trends in follicular development, atresia and corpus luteum regression: role for apoptosis. *Reprod Biomed Online* 11:93–103.

SANTOS, H.B.; RIZZO, E.; BAZZOLI, N.; SATO, Y.; MORO, L. (2005) Ovarian regression and apoptosis in the South American teleost *Leporinus taeniatus* Lütken (Characiformes, Anostomidae) from the São Francisco Basin. *J Fish Biol* 67:1446–59.

SANTOS, H.B.; THOMÉ, R.G.; ARANTES, F.P.; SATO, Y.; BAZZOLI, N.; RIZZO, E. (2008a) Ovarian follicular atresia is mediated by heterophagy, autophagy, and apoptosis in *Prochilodus argenteus* and *Leporinus taeniatus* (Teleostei: Characiformes). *Theriogenology* 70(9):1449–60.

SANTOS, H.B.; SATO, Y.; MORO, L.; BAZZOLI, N.; RIZZO, E. (2008b) Relationship among follicular apoptosis, integrin β1 and collagen type IV during early ovarian regression in the teleost *Prochilodus argenteus* after induced spawning. *Cell Tissue Res* 332:159–170.

SUNDARESAN, N.R.; SAXENA, V.K.; SASTRY, K.V.H.; ANISH, D.; SAXENA, M.; NAGARAJAN, K.; AHMED, K.A. (2007) Nitric oxide: a possible mediator of ovulation and postovulatory follicle regression in chicken. *Anim Reprod Sci* 101:351–357.

TACON, P.; NDIAYE, P.; CAUTY, C.; LE MENN, F.; JALABERT, B. (1996) Relationships between the expression of maternal behaviour and ovarian development in the mouthbrooding cichlid fish *Oreochromis niloticus*. *Aquaculture* 146:261–275.

THOMÉ, R.G.; SANTOS, H.B.; ARANTES, F.P.; PRADO, P.S.; DOMINGOS, F.F.T.; SATO, Y.; BAZZOLI, N.; RIZZO, E. (2006) Regression of post-ovulatory follicles in

Prochilodus costatus Valenciennes, 1850 (Characiformes, Prochilodontidae). *Braz J Morphol Sci* 23:495–500.

THOMÉ, R.G.; SANTOS, H.B.; ARANTES, F.P.; DOMINGOS, F.F.T.; BAZZOLI, N.; RIZZO, E. (2009) Dual roles for autophagy during follicular atresia in fish ovary. *Autophagy* 5: 117-119.

THOMÉ, R.G.; SANTOS, H.B.; SATO, Y.; RIZZO, E.; BAZZOLI, N. (2010). Distribution of laminin β2, collagen type IV, fibronectin and MMP-9 in ovaries of the teleost fish. *J Mol Hist* 41:215–224.

THOMÉ, R.G.; DOMINGOS, F.F.T.; SANTOS, H.B.; MARTINELLI, P.M.; SATO, Y.; RIZZO, E.; BAZZOLI N. (2012) Apoptosis, cell proliferation and vitellogenesis during the folliculogenesis and follicular growth in teleost fish. *Tissue Cell* 44:54–62.

THOMPSON, C.B. (1995) Apoptosis in the pathogenesis and treatment of disease. *Science* 267:1456–1462.

TYLER, C.R & SUMPTER, J.P. (1996) Oocyte growth and development in teleosts. *Rev Fish Biol Fish* 6:287–318.

VELENTZAS, A.D.; NEZIS, I.P.; STRAVOPODIS, D.J.; PAPASSIDERI, I.S.; MARGARITIS, L.H. (2007) Apoptosis and autophagy function cooperatively for the efficacious execution of programmed nurse cell death during *Drosophila virilis* oogenesis. *Autophagy* 3:130–132.

YARON, Z. & LEVAVI-SIVAN, B. (2011) Endocrine regulation of fish reproduction. In: Farrel AP. (ed). *Encyclopedia of fish physiology: from genome to environment*. San Diego: Academic Press, Elsevier, pp. 1500–1508.